ornl

OAK RIDGE NATIONAL LABORATORY

UNION CARBIDE

ORNL-5899

Elevated-Temperature Tensile and Creep-Rupture Behavior of Alloy 800H/ERNiCr-3 Weld Metal/2 ¼ Cr-1 Mo Steel Dissimilar-Metal Weldments

R. L. Klueh
J. F. King

METALS and CERAMICS
ENERGY
RESEARCH
DEVELOPMENT
OAK RIDGE NATIONAL LABORATORY

[redacted]

This document does not contain UCNI, ECI, or other unclassified sensitive information and has been approved for release to the public by:

David R. Hamrin 1/19/2010
David R. Hamrin, ORNL Classification Officer Date

OPERATED BY
UNION CARBIDE CORPORATION
FOR THE UNITED STATES
DEPARTMENT OF ENERGY

Printed in the United States of America. Available from
the U.S. Department of Energy
Technical Information Center
P.O. Box 62, Oak Ridge, Tennessee 37830

ORNL-5899
Dist. Category UC-79Th,
-Tk, -Tr
Task OR-1.3, "Mechanical
Properties Design Data

METALS AND CERAMICS DIVISION

ELEVATED-TEMPERATURE TENSILE AND CREEP-RUPTURE BEHAVIOR OF ALLOY 800H/ERNiCr-3 WELD METAL/2 1/4 Cr-1 MO STEEL DISSIMILAR-METAL WELDMENTS

R. L. Klueh and J. F. King

Date Published - November 1982

Prepared by the
OAK RIDGE NATIONAL LABORATORY
Oak Ridge, Tennessee 37830
operated by
UNION CARBIDE CORPORATION
for the
U.S. Department of Energy
Under Contract No. W-7405-eng-26

CONTENTS

ELEVATED-TEMPERATURE TENSILE AND CREEP-RUPTURE BEHAVIOR OF ALLOY 800H/ERNiCr-3 WELD METAL/2 1/4 Cr-1 Mo STEEL DISSIMILAR-METAL WELDMENTS*

R. L. Klueh and J. F. King

ABSTRACT

Tensile tests at room temperature, 510, and 566°C and creep-rupture tests at 510°C were made on specimens taken from dissimilar-metal welds made on isothermally annealed 2 1/4 Cr-1 Mo steel and mill-annealed alloy 800H plates joined with ERNiCr-3 filler metal. The specimens were machined so that the gage length contained all three alloys; the weld metal was in the center of the gage section. The weldments were tested under several postweld heat treatment (PWHT) and aging conditions. The PWHT conditions were 1 h at 677°C, 1 h at 732°C, and 10 h at 732°C. Specimens in each of the PWHT conditions were tested unaged and after aging 1000 h at 510°C and 2000 h at 566°C. Tests were also made on specimens taken from a dissimilar joint made from large-diameter pipe prototypic of that in the demonstration breeder reactor plant. For this weld, tensile tests were made at room temperature and 593°C, and creep rupture tests were made in air and flowing argon at 593°C.

Ductile cup-cone tensile failures occurred in the 2 1/4 Cr-1 Mo steel base metal well removed from the weld fusion line, as expected from the relative base metal properties. For creep at 510°C and rupture lifetimes of up to about 2000 h, failure also occurred in the 2 1/4 Cr-1 Mo steel base metal. Three low-stress tests failed in the 2 1/4 Cr-1 Mo steel with low ductility in over 7500 h within 10 μm of the fusion line. The fracture microstructure for this interface-type failure was similar to that of dissimilar-metal weld failures in the tubing of operating fossil-fired steam plants. A similar type of failure was noted for the low-stress tests at 593°C.

Metallographic studies showed that the interface-type failures resulted by a previously proposed mechanism that involves the formation of a chromium-depleted region parallel to the fusion line. An oxide notch that forms in the 2 1/4 Cr-1 Mo steel in a chromium-depleted region (chromium affects oxidation resistance) very near the fusion line nucleates a grain-boundary crack, which eventually leads to a low-ductility fracture.

*Work performed under DOE/BTR AF 15 40 10 3, Task OR-1.3, Mechanical Properties Design Data.

INTRODUCTION

The intermediate heat exchanger of the Clinch River Breeder Reactor Plant (CRBRP) is to be constructed from an austenitic stainless steel and the steam generators from the low-alloy ferritic 2 1/4 Cr-1 Mo steel. Thus, a welded transition joint between these two units will be required. The problems inherent in such joints have long been recognized.[1-5] Recently the utility industry has experienced a rash of transition-joint failures in fossil-fired steam plants. These failures often occur after 15 to 20 years of operation, well before the lifetime of the tubing has been exhausted.

Because of the economic consequences of a power plant shutdown, the need for an improved dissimilar-metal joint is obvious. The consequences of the failure of a joint in a breeder reactor, where sodium is involved, are even greater than for a fossil-fired plant. Thus, design studies have sought the best type of joint for this application. This investigation is part of that effort.

The great majority of austenitic-ferritic, dissimilar-alloy weld failures that have occurred in service[6] or in test programs[1-5] failed in the ferritic alloy. In most of the service failures, the ferritic alloy was 2 1/4 Cr-1 Mo steel tubing and piping — primarily because most fossil-fired power plants are constructed with this widely used steel.

Factors that contribute to dissimilar-alloy weld failures in fossil-fired plants have long been understood.[1-5] Tucker and Eberle[4] summarized them as (1) cyclic thermal stresses, (2) low oxidation resistance of the low-alloy ferritic steel, (3) carbon migration, and (4) metallurgical deterioration caused by elevated-temperature exposure.

During the operation of a power plant, numerous startups and shutdowns occur. Because of the differences in coefficients of thermal expansion for the three components in a joint (the ferritic and austenitic alloys and the weld metal), the startups and shutdowns generate thermal stresses within the joint. The cyclic stresses superimposed on the residual welding stresses and internal steam pressure are believed to be the ultimate cause of the failure. Also, an external load may act on the joint.

Although it has generally been thought that a cyclic stress is required to produce this type of dissimilar-metal weld failure, Nicholson recently produced such failures in a creep-rupture test.[7] We agree, however, that in an operating steam plant the stresses responsible for dissimilar-metal weld failures are due to the thermal cycling when the plant is started and stopped.

In conjunction with our studies to develop an improved dissimilar-alloy weld joint for liquid-metal fast-breeder reactor applications, we have examined the problem for joints made with 2 1/4 Cr-1 Mo steel welded to an austenitic stainless steel with austenitic stainless steel and high-nickel weld filler metals.[8] Our observations were combined with previous results to develop a mechanism by which the interface microstructure forms during welding, to learn how it evolves during elevated-temperature service, and to learn how this microstructure leads to failure. The chief new feature of the proposed mechanism was the formation of a chromium-depleted region that is prone to enhanced oxidation and eventually leads to crack nucleation and propagation. The mechanism is summarized below.

Because of the lower carbon activity in the weld metal, during welding carbon diffuses from the 2 1/4 Cr-1 Mo steel toward the weld metal. Carbon loss in the 2 1/4 Cr-1 Mo steel results in the dissociation of carbides and grain boundary migration. The resulting 2 1/4 Cr-1 Mo steel microstructure near the weld interface has prior-austenite grain boundaries parallel to the fusion line (the distance of these grain boundaries from the fusion line is a measure of the extent of decarburization). After the carbides in the grain boundaries dissociate, regions high in chromium are left behind. At the welding temperature, these regions transform to δ-ferrite and grow at the expense of the chromium in the matrix.

When cooled from the welding temperature and while in service, the high-chromium regions in the grain boundaries carburize. As the carbide particles grow, the matrix immediately adjacent to the grain boundaries is further depleted in chromium. The lower chromium concentration in the vicinity of the prior-austenite grain boundaries leads to lower oxidation resistance of the 2 1/4 Cr-1 Mo steel. Inevitably, an oxide notch forms on the external surface (inner or outer) in this chromium-depleted region (the chromium concentration in solution in the matrix and grain boundaries determines the oxidation resistance of the 2 1/4 Cr-1 Mo steel).

We have postulated that a fatigue crack nucleates below the oxide notch.[8] Nucleation is caused by external-loading stresses superimposed on the internal tube pressure and the cyclic thermal stresses during heating and cooling of the fossil-fired plant. The thermal stresses are due to the differences in coefficients of thermal expansion of the materials making up the joint. The difference in external loads (i.e., bending stresses and welding stresses) on different tubes explains why some tubes fail and other similar ones do not.[8]

Once a crack is nucleated, it will propagate in the chromium-depleted region. Crack propagation occurs under the influence of the external load, the internal tube pressure, and the cyclic thermal stresses; it can also be aided by the stress generated by the large volume of oxide formed within a crack. More importantly, this region has lower strength because of carbon loss during welding and service, so crack propagation through this region is easier.

Of crucial importance to the proposed mechanism is the enrichment of chromium in the prior-austenite grain boundaries of the 2 1/4 Cr-1 Mo steel heat-affected zone. By the use of microprobe analysis, we showed that the carbides within the grain boundaries are enriched in chromium relative to the matrix immediately adjacent to the grain boundaries. We also cite work of Apblett et al.,[9] who showed that δ-ferrite can form in these grain boundaries during welding. According to those authors, δ-ferrite results when alloy carbides (chromium-rich carbides) dissociate during welding, giving rise to a region sufficiently enriched in alloy content to close the gamma loop. Since the previous report,[8] Doig and Flewitt[10] produced further evidence for chromium enrichment. They measured chromium concentrations of about 10% at prior-austenite grain boundaries of quenched 2 1/4 Cr-1 Mo steel. Most of the concentration change was estimated to be restricted to about 20 nm of the grain boundaries.

Based on the proposed failure mechanism, several possible solutions were proposed.[8] Elimination of external loading stresses is the most obvious. Others include transition pieces (spool pieces) between the tubes to lower the thermal stresses and oxidation-resistant coatings on the external surfaces of the welds. In addition to proposing a spool piece that would lower thermal stresses (the CRBRP solution), the proposed failure mechanism leads to a possible alternative transition-piece solution. We proposed a chromium-molybdenum steel transition piece with higher chromium concentration than 2 1/4% Cr. Besides keeping sufficient chromium available to maintain oxidation resistance and thus avoid oxide notch formation, the higher chromium concentration of such a spool piece may also lower the amount of carbon transferred during welding and service (perhaps a carbon-stabilized chromium-molybdenum steel could be used).

Design studies have sought the best method to minimize the possibility of failure of the transition joint of the CRBRP.[11,12] Instead of making the transition with a single weld directly from the 2 1/4 Cr-1 Mo steel of the steam generator to the type 316 stainless steel of the intermediate heat exchanger, a spool piece is to be used.[12] The material for the spool piece is chosen to provide a more gradual change in the coefficients of thermal expansion for the materials in the joint than is present for a joint that goes directly from the 2 1/4 Cr-1 Mo steel to the type 316 stainless steel. Such a trimetallic joint should minimize the thermal stresses during startup and shutdown.

Alloy 800H has been proposed as the spool piece. Figure 1 shows a schematic diagram of the proposed CRBRP transition joint and the respective coefficients of thermal expansion for each material involved in the joint. The more gradual change in coefficient of thermal expansion in going from the ferritic to the austenitic tube is quite apparent. The improvement in thermal stresses generated in this trimetallic joint over the bimetallic joint has been demonstrated by finite-element analysis.[12]

To learn about the elevated-temperature deformation behavior of the proposed joint, tensile, creep, and fatigue studies were conducted on material taken from simulated transition-joint weldments. This report presents the results of the tensile and creep studies.

ORNL–DWG 75–7748R2

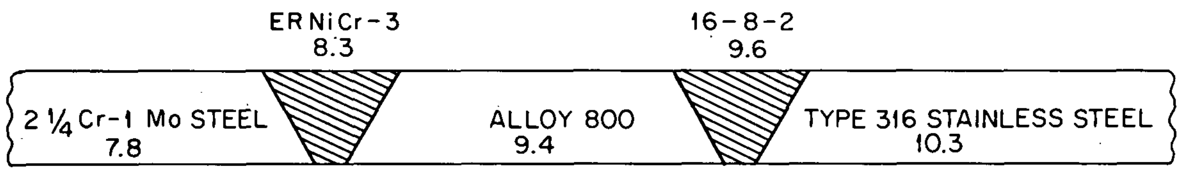

Fig. 1. Schematic diagram of transition joint with alloy 800H spool piece proposed for liquid-metal fast-breeder reactor application. Mean coefficients of thermal expansion from 21 to 538°C (70 to 1000°F) for each material in the joint are shown. The units are 10^{-6}/°F. The corresponding values are 13.9, 14.9, 16.9, 17.3, and 18.5 × 10^{-6}/°C.

EXPERIMENTAL

The hot-wire gas tungsten arc welding process was selected for joining the dissimilar-metal transition joints to be used in the CRBR. This process was chosen for its high rate of metal deposition, low weld-dilution potential, and high-quality weld deposits. As in conventional gas tungsten arc welding, an arc is established between the tungsten electrode and the work. In the hot-wire process the filler metal is electrically heated (resistance heated) and added to the weld puddle in the molten state. In contrast to the cold-wire process, in which the filler wire is melted by the arc, the hot-wire process requires that the welding arc provide only sufficient heat to maintain puddle fluidity for forming the weld bead and melting the base metal to ensure side-wall fusion. High-deposition-rate welding and low weld-metal dilution result.

The weldments for this study were 19-mm-thick plates of 2 1/4 Cr-1 Mo steel and alloy 800H joined with AWS specification A5.14 Class ERNiCr-3 filler metal. A joint geometry with a 30°-included-angle V-groove with a 12.7-mm root opening and a backing strip was used for these welds. Before welding, the 2 1/4 Cr-1 Mo steel plates had been given an isothermal anneal heat treatment (1 h at 927°C, furnace cool to 704°C, hold for 2 h, and air cool). The alloy 800H was used in the mill solution-annealed condition. The welding procedure required eight weld passes to complete the joint with nominal welding parameters of 350 A, 12 V, and a travel speed of 1.7 mm/s.

Composite alloy 800H/ERNiCr-3 weld metal/2 1/4 Cr-1 Mo steel specimens taken from the weldments were tensile tested at room temperature, 510, and 566°C. The specimens contained all three materials in the 6.4-mm-diam × 63.5-mm-long (0.25 × 1.25 in.) reduced section (Fig. 2). Creep-rupture tests were made at 510°C in the aged and unaged conditions (Table 1) after various postweld heat treatments (PWHTs). The 510°C test temperature is near the highest operating temperature of joints in the CRBRP. The PWHTs used were 1 h at 677°C, 1 h at 732°C, and 10 h at 732°C. Specimen blanks with the given PWHT were aged 1000 h at 510°C and 2000 h at 566°C. The objective of the creep-rupture tests was the generation of stress-rupture curves to about 1000 h for all PWHT and aging conditions and to approximately 10,000 h for the unaged and aged weldment specimens with the 1 h at 732°C PWHT (Table 1).

Table 1. Proposed test matrix for 510°C creep-rupture tests of 2 1/4 Cr-1 Mo/ERNiCr-3/alloy 800H composite specimens

Aging treatment	Proposed rupture life (h) for each PWHT		
	677°C/1 h	732°C/1 h	732°C/10 h
None	100	100	100
	500	500	500
	1,000	1,000	1,000
		10,000	
510°C/1,000 h	100	100	100
	500	500	500
	1,000	1,000	1,000
		10,000	
566°C/2,000 h	100	100	100
	500	500	500
	1,000	1,000	1,000
		10,000	

Y-183604

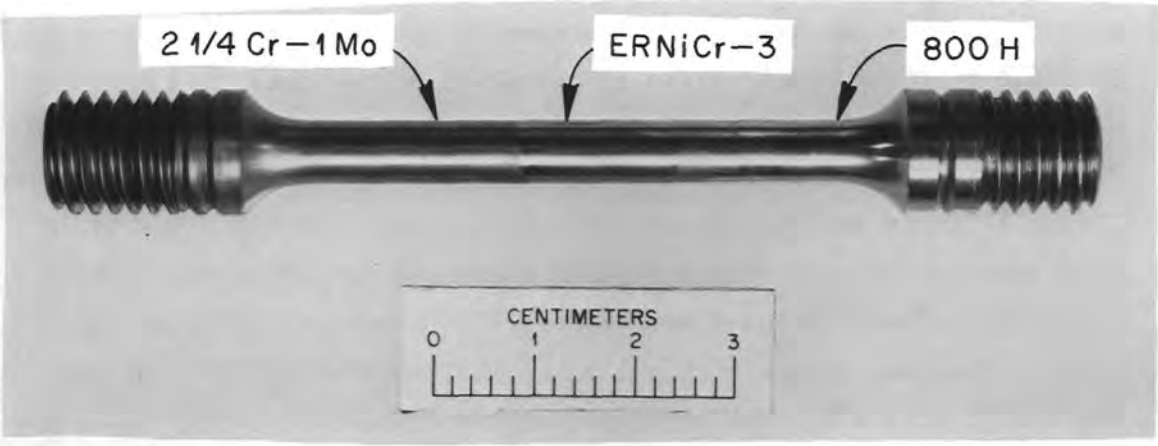

Fig. 2. Composite test specimen showing the three materials contained in the gage section.

Although most of the creep-rupture tests were made at 510°C on composite specimens taken from the plate welds, a second series of weldment specimens were tested at 593°C. These tests were made in conjunction with the General Electric Transition Joint Life Test (TLJT) Program.[13,14] In that program accelerated-life tests of large-diameter piping (similar in size to that in the CRBRP transition joint) are being conducted. Pipes 0.46 m in diameter are fabricated to contain five transition welds, which join combinations of 2 1/4 Cr-1 Mo steel, alloy 800H, and type 316 stainless steel (Fig. 3). These welded pipes then become the test specimens for accelerated rupture tests at 593°C under conditions that are predicted by stress analysis to cause failure (crack initiation) in two years or less.[13,14]

Tensile and creep-rupture test specimens for our study were machined from a piece of TLJT alloy 800H pipe welded to 2 1/4 Cr-1 Mo steel with ERNiCr-3 weld metal according to welding procedures prototypic for the CRBRP transition joint.[13] Tensile tests were made in air room temperature and 593°C. Creep-rupture tests were made at 69, 83, and 97 MPa at 593°C. Two tests were made at each stress, one in air, the other in flowing argon.

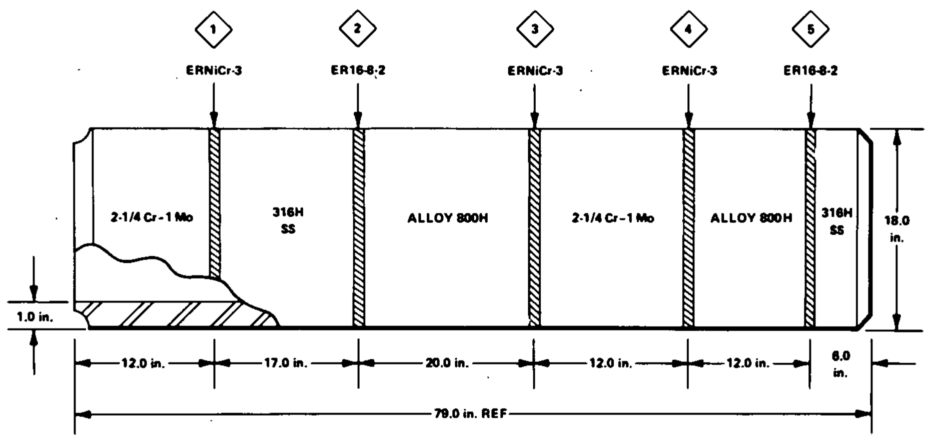

Fig. 3. Schematic diagram of the test specimen used in the General Electric Transition Joint Life Test. Dimensions in millimeters are OD, 457; wall thickness, 25; length sections, left to right, 205, 432, 508, 305, 305, and 152; total length, 2007. Drawing from General Electric Company.

Tensile tests were made on an Instron machine with a crosshead speed of 8.5 µm/s, which gave a nominal strain rate of 4×10^{-5}/s. Creep-rupture tests were made in air in constant-load lever-arm creep frames. During test the specimens were heated in a resistance tube furnace, and the temperature was monitored and controlled by three Chromel vs Alumel thermocouples attached to the specimen gage length. Temperature was controlled to ±1°C with a temperature variation along the gage length of less than ±2°C. Elongations were determined with mechanical extensometers attached to the specimen grips, and the specimen elongation was read periodically on a dial gage.

EXPERIMENTAL RESULTS

TENSILE RESULTS

Tensile tests were made on dissimilar-metal weld specimens and specimens of alloy 800H and 2 1/4 Cr-1 Mo steel base metals at room temperature, 510, and 566°C for each PWHT and aging condition (Tables 2–4). The 0.2% yield strength and ultimate tensile strength as functions of temperature for the aged and unaged weldment and base metal specimens given PWHTs of 1 h at 677°C, 1 h at 732°C, and 10 h at 732°C are given in Figs. 4 through 6.

Table 2. Tensile properties of annealed 2 1/4 Cr-1 Mo steel base metal

PWHT		Age		Test temperature	Strength (MPa)		Reduction of area
(h)	(°C)	(h)	(°C)	(°C)	Yield	Ultimate	(%)
1	677	0		21	249	460	59.2
				510	176	384	61.7
				566	159	275	77.7
1	732	0		21	270	466	61.9
				510	181	426	60.3
				566	170	315	75.8
10	732	0		21	250	460	60.2
				510	169	394	62.0
				566	155	276	77.5
1	677	1000	510	21	209	459	61.1
				510	158	322	68.6
				566	156	264	87.0
1	732	1000	510	21	219	452	62.9
				510	163	343	67.7
				566	154	273	80.6
10	732	1000	510	21	208	451	62.3
				510	150	323	70.2
				566	141	258	80.9
1	677	2000	566	21	188	460	71.9
				510	151	293	79.9
				563	139	235	87.6
1	732	2000	566	21	185	454	62.6
				510	150	297	71.7
				566	140	244	86.5
10	732	2000	566	21	176	449	63.2
				510	141	289	69.6
				566	129	222	81.0

Table 3. Tensile properties of composite dissimilar-metal 2 1/4 Cr-1 Mo steel/ERNiCr-3/alloy 800H weld specimens

(All specimens fractured in the 2 1/4 Cr-1 Mo steel base metal)

PWHT		Age		Test temperature	Strength (MPa)		Reduction of area
(h)	(°C)	(h)	(°C)	(°C)	Yield	Ultimate	(%)
1	677	0		21	240	470	69.9
				510	171	370	75.1
				566	168	279	84.4
1	732	0		21	255	470	70.1
				510	173	402	69.5
				566	160	296	83.7
10	732	0		21	251	456	68.2
				510	169	385	71.2
				566	157	293	83.2
1	677	1000	510	21	216	470	72.5
				510	173	370	79.5
				566	163	279	86.5
1	732	1000	510	21	209	470	69.3
				510	166	402	79.3
				566	157	296	85.9
10	732	1000	510	21	202	456	70.7
				510	166	385	79.4
				566	155	293	87.7
1	677	2000	566	21	216	474	70.3
				510	170	297	82.4
				566	153	240	87.6
1	732	2000	566	21	209	463	69.7
				510	169	300	79.3
				566	152	230	88.2
10	732	2000	566	21	213	457	72.0
				510	167	295	80.4
				566	150	229	87.4

Table 4. Tensile properties of alloy 800H base metal

PWHT (h)	PWHT (°C)	Age (h)	Age (°C)	Test temperature (°C)	Strength (MPa) Yield	Strength (MPa) Ultimate	Reduction of area (%)
1	677	0		21	229	550	59.0
				510	145	463	47.7
				566	142	450	41.2
1	732	0		21	196	538	58.3
				510	121	459	42.6
				566	122	435	48.1
10	732	0		21	215	562	46.6
				510	130	465	41.7
				566	131	437	45.3
1	677	1000	510	21	225	556	54.7
				510	154	460	43.6
				566	161	438	45.5
1	732	1000	510	21	208	550	57.2
				510	141	452	46.6
				566	127	439	48.8
10	732	1000	510	21	210	560	48.9
				510	141	462	40.8
				566	153	443	35.3
1	677	2000	566	21	262	626	52.0
				510	196	506	42.6
				566	189	464	37.2
1	732	2000	566	21	243	623	46.0
				510	177	494	46.2
				566	171	460	40.0
10	732	2000	566	21	247	627	38.3
				510	183	501	41.8
				566	201	463	32.8

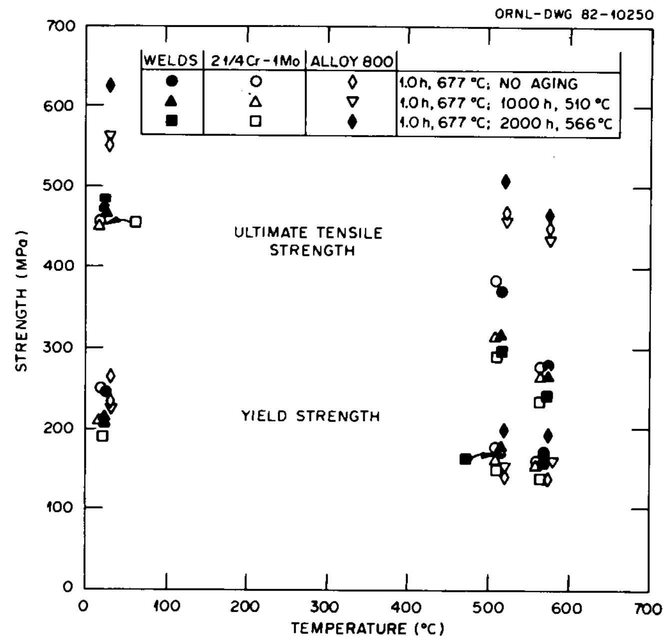

Fig. 4. The 0.2% yield strength and ultimate tensile strength as functions of test temperature for the unaged and aged composite weldment specimens and 2 1/4 Cr-1 Mo steel and alloy 800H base metal specimens postweld heat treated 1 h at 677°C.

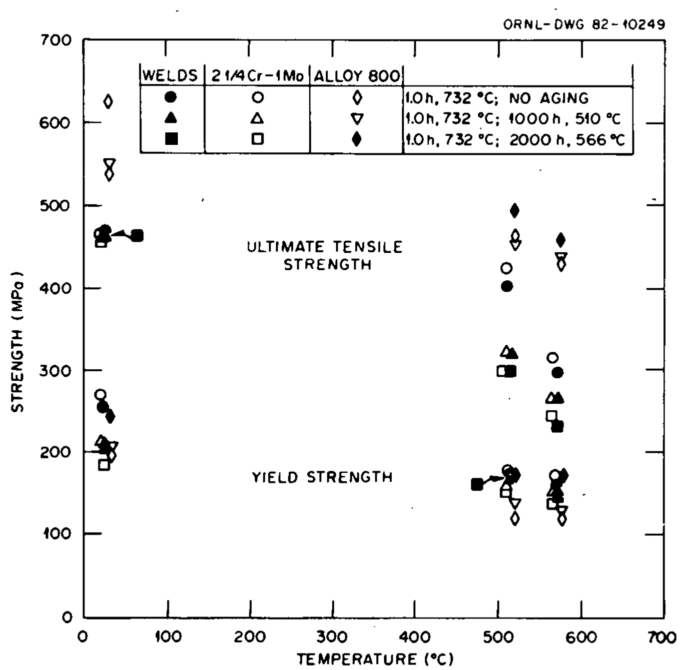

Fig. 5. The 0.2% yield strength and ultimate tensile strength as functions of test temperature for the unaged and aged composite weldment specimens and 2 1/4 Cr-1 Mo steel and alloy 800H base metal specimens postweld heat treated 1 h at 732°C.

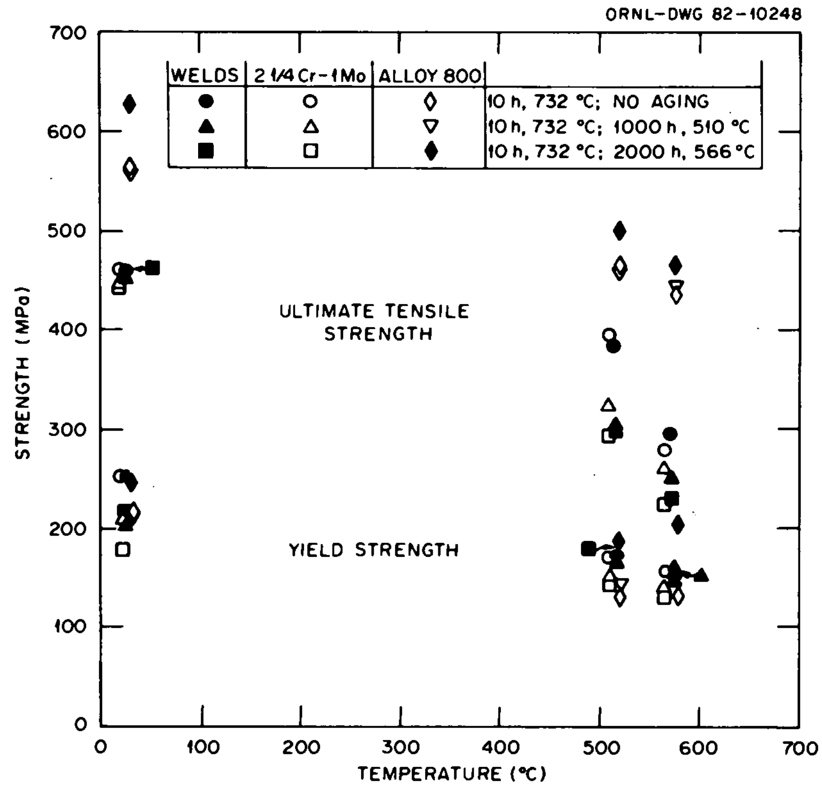

Fig. 6. The 0.2% yield strength and ultimate tensile strength as functions of test temperature for the unaged and aged composite weldment specimens and 2 1/4 Cr-1 Mo steel and alloy 800H base metal specimens postweld heat treated 10 h at 732°C.

For all PWHT and aging conditions, there was little difference in the yield strengths of the weldment specimens, the alloy 800H base metal, and the 2 1/4 Cr-1 Mo steel base metal. Previous tensile studies on ERNiCr-3 weld metal specimens given a PWHT of 1 h at 732°C showed this alloy to have a yield strength almost twice the values found for the three types of specimens tested here.[15]

The ultimate tensile strengths for the dissimilar-metal welds were similar to those for the 2 1/4 Cr-1 Mo steel; the values for alloy 800H were considerably greater than those for the other two types of specimens. The ultimate tensile strength values for ERNiCr-3 weld metal are similar to those for alloy 800H.[15]

The effect of thermal aging on the composite weldment specimens is seen in Fig. 7. At room temperature thermal aging affected only the

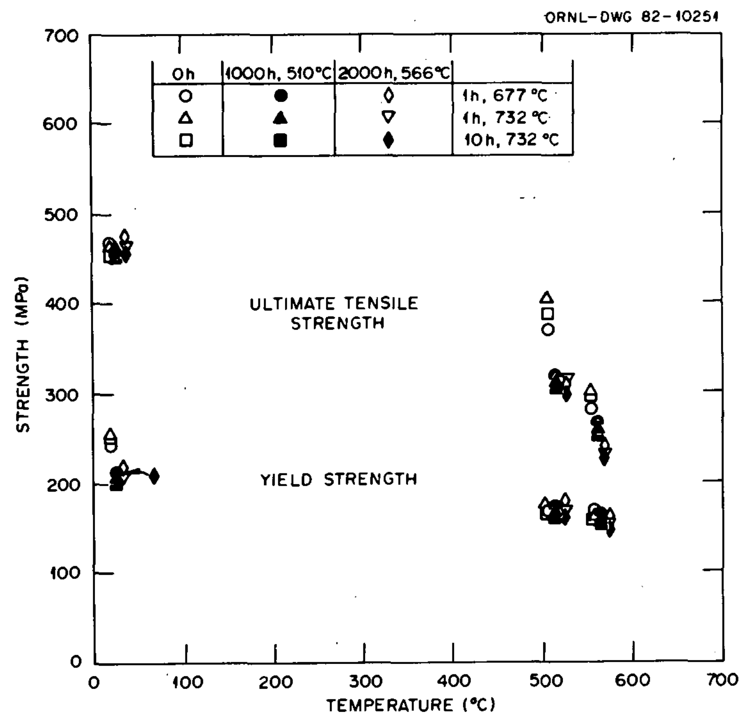

Fig. 7. The 0.2% yield strength and ultimate tensile strength of the composite weldment specimens for all postweld heat treatment and aging conditions.

yield strength, but at the two elevated temperatures thermal aging affected the ultimate tensile strength, with the relative effect being greater at 510°C. Note that in the unaged condition the weldment with the PWHT of 1 h at 732°C was usually the strongest, followed by the one that received 10 h at 732°C and then the one receiving the 1 h at 677°C. We would have expected the last one to have been the strongest.

All the dissimilar-metal weld specimens fractured in the 2 1/4 Cr-1 Mo steel base metal. The failures were typical ductile cup-cone type fractures. In all cases the failures occurred at some distance (>13 mm) from the weld metal/2 1/4 Cr-1 Mo steel fusion line and did not appear to be influenced by the weld metal.

Although the failure occurred in the 2 1/4 Cr-1 Mo steel base metal, the alloy 800H and the ERNiCr-3 weld metal portions of the gage section were also deformed (Table 5). The deformation varied along the gage section, and only the minimum values are given in Table 5. This deformation is not unexpected when the similarity of the yield strengths

Table 5. Minimum diameter of alloy 800H and ERNiCr-3 portions of composite specimens

(The amount of deformation varied along the specimen. Original diameter was approximately 6.35 mm.)

PWHT		Age		Test temperature	Minimum diameter (mm)	
(h)	(°C)	(h)	(°C)	(°C)	Alloy 800H	ERNiCr-3
1	677	0		26	5.79	5.82
				510	5.74	5.94
				566	6.15	6.32
1	732	0		26	5.82	5.72
				510	5.64	5.69
				566	6.07	6.27
10	732	0		26	5.97	5.77
				510	5.89	5.77
				566	6.22	6.22
1	677	1000	510	26	5.16	5.87
				510	6.02	6.20
				566	6.20	6.35
1	732	1000	510	26	5.84	5.84
				510	5.94	6.27
				566	6.12	6.35
10	732	1000	510	26	6.05	5.87
				510	6.20	6.27
				566	6.17	6.30
1	677	2000	566	26	6.02	6.32
				510	6.25	6.32
				566	6.35	6.35
1	732	2000	566	26	6.35	5.99
				510	6.35	6.20
				566	6.35	6.35
10	732	2000	566	26	6.07	6.32
				510	6.27	6.35
				566	6.35	6.35

for the three materials is considered. Alloy 800H and ERNiCr-3 deformed most in the alloy 800H portion of the specimen that was tested at room temperature after the PWHT of 1 h at 677°C and then aged 1000 h at 510°C. Reduction of area in this case was approximately 30%. For all other tests the deformation was considerably less. The amount of deformation depended on the PWHT and aging conditions. The aged ERNiCr-3 weld metal displayed less deformation than the unaged material. This was also true for the alloy 800H, but only when aged at 566°C.

CREEP-RUPTURE TEST RESULTS

Creep-rupture tests were made at 510°C on specimens with each PWHT and aging condition (Table 6). At least three tests were made for each heat-treatment condition, so a stress-rupture curve could be determined to approximately 2000 h (Fig. 8). For the three specimens given the 1-h PWHT at 732°C (unaged, aged 1000 h at 510°C and 2000 h at 566°C), we ran tests that were predicted to rupture in approximately 10,000 h, allowing an extension of the stress-rupture curves for these conditions (Fig. 9).

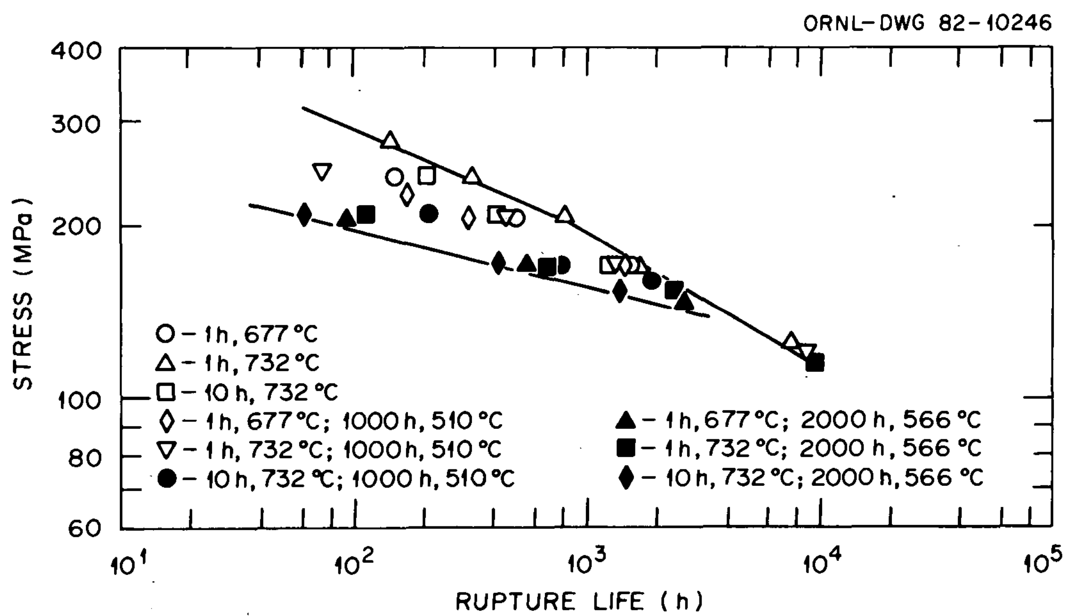

Fig. 8. Stress-rupture results for composite weldment specimens tested at 510°C.

Table 6. Creep-rupture properties of composite 2 1/4 Cr-1 Mo/ERNiCr-3/alloy 800H specimens at 510°C

PWHT		Age		Stress (MPa)	Rupture time (h)	Reduction of area (%)	Minimum creep rate (%/h)
(h)	(°C)	(h)	(°C)				
1	677	0		241	155.5	76.9	0.0139
				207	486.4	79.4	0.00527
				172	1535.6	83.1	0.00183
1	732	0		276	146.9	67.1	0.0101
				241	317.8	71.5	0.00386
				207	809.2	72.1	0.00135
				172	1681.3	75.8	0.000113
				134	7823.4	6.8	0.000556
10	732	0		241	203.9	75.4	0.00550
				207	428.4	78.6	0.00260
				172	1270.6	81.4	0.00110
1	677	1000	510	224	173.9	81.5	0.0279
				207	310.9	79.3	0.0149
				172	1508.4	81.4	0.00330
1	732	1000	510	241	74.2	67.6	0.0752
				207	444.6	72.1	0.0113
				172	1296.7	75.9	0.00434
				131	8768.4	7.7	0.000426
10	732	1000	510	207	217.0	79.6	0.0254
				172	795.0	81.1	0.00813
				159	1948.0	82.1	0.00369
1	677	2000	566	207	96.8	81.1	0.0767
				172	560.9	82.5	0.0146
				148	2684.4	84.2	0.00272
1	732	2000	566	207	116.9	70.9	0.0520
				172	698.3	77.0	0.00940
				152	2410.6	76.5	0.00234
				124	9519.8	15.2	0.000385
10	732	2000	566	207	63.0	79.2	0.0967
				172	427.4	83.5	0.0163
				152	1313.7	83.3	0.00520

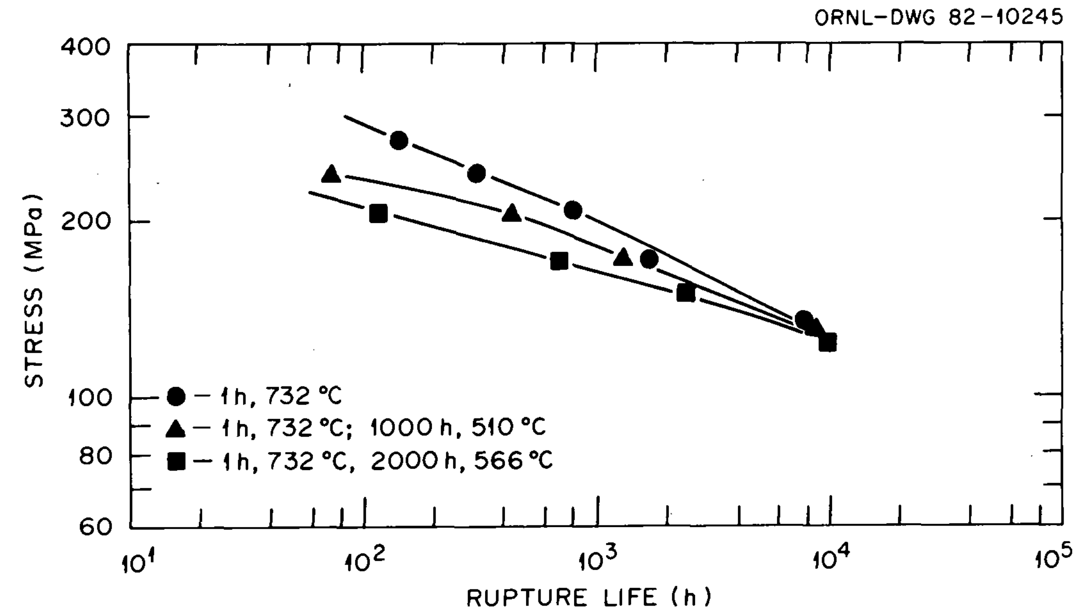

Fig. 9. Stress-rupture curves at 510°C for aged and unaged composite weldment specimens that were postweld heat treated for 1 h at 732°C.

For rupture times of 1000 to 2000 h, the stress-rupture data could generally be fit by a straight line (Figs. 8 and 9). All the data were contained between the stress-rupture curve for the specimens given a PWHT of 1 h at 732°C (no age), which defined the strongest material, and the curve for the specimens given the 10 h at 732°C PWHT and then aged 2000 h at 566°C, which defined the weakest material. This latter heat treatment is the most severe and would be expected to have the largest effect on the strength of 2 1/4 Cr-1 Mo steel, the component of the composite specimen in which failure (and most deformation) occurred. In the case of the strongest specimens, apparently the 1 h at 732°C PWHT has less effect on the strength than the 1 h at 677°C. This agrees with the tensile data for the 2 1/4 Cr-1 Mo steel base metal (Table 3). Because none of this heat of 2 1/4 Cr-1 Mo steel was tested in the isothermally annealed condition, we could not determine whether the 1 h at 732°C strengthened the isothermally annealed steel or had a smaller effect on the loss of strength than the other two PWHT conditions. Although creep-rupture strengths vary with heat-treatment conditions, if all the data in Fig. 8 were fit with curves the curves would converge at long rupture times (low stresses).

When the three long-time rupture datum points are included for their respective creep-rupture curves, the curves contain downward curvature beyond 1000 to 2000 h (Fig. 9). For the three long-time tests, the PWHT and aging appear to have very little effect on the strength. All three of the long-time tests ruptured with a considerably smaller reduction of area than did the higher-stress tests (Table 6). Although all other specimens ruptured with a reduction of area greater than 65% and no apparent effect of stress (rupture life), the three long-time tests ruptured with reduction of area values of 6.8, 7.7, and 15.2%, respectively, for specimens that were unaged, aged 1000 h at 566°C, and aged 2000 h at 566°C (all three specimens had a PWHT of 1 h at 732°C).

Visual inspection of the fractured specimens indicated that all but the three long-time rupture tests failed essentially midway in the 2 1/4 Cr-1 Mo steel portion of the gage section, between the ERNiCr-3 weld metal and the specimen shoulder (Fig. 10). The fractures were ductile

Y-183602

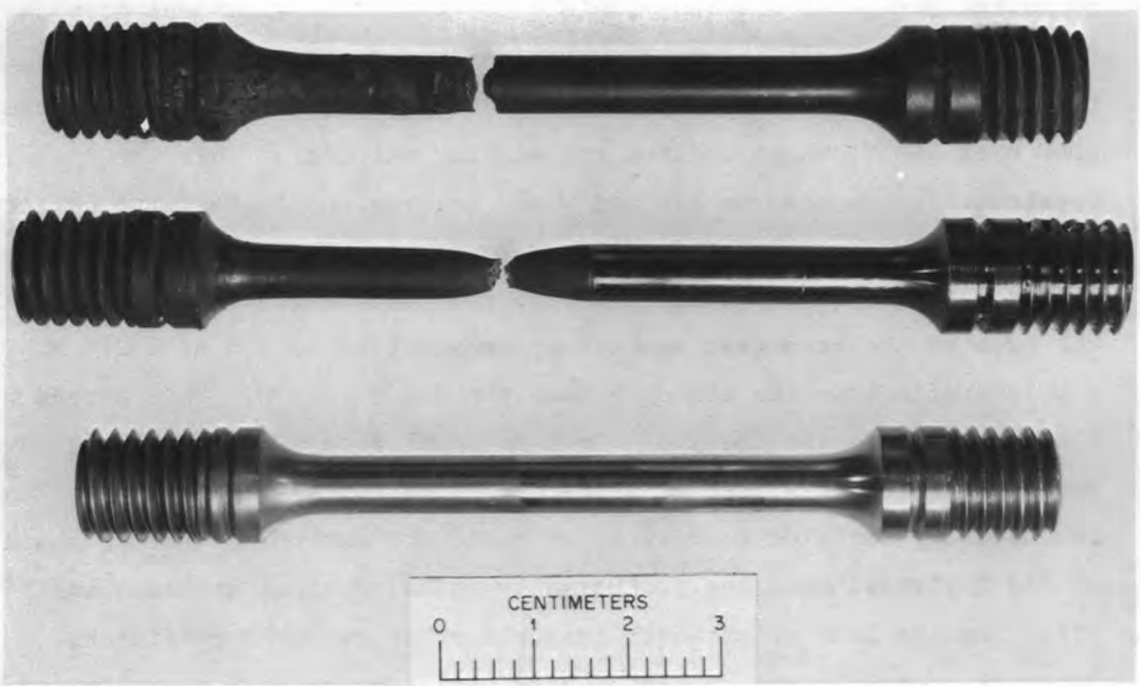

Fig. 10. Different fracture modes. Bottom specimen is untested, middle one is a high-ductility fracture in the 2 1/4 Cr-1 Mo steel base metal, and the top is a low-ductility failure near the fusion line.

cup-cone type failures well removed from the weld fusion line, and the weld did not appear to be involved (the fractures were similar to the tensile test failures). On the specimen postweld heat treated 1 h at 677°C and aged 2000 h at 566°C (rupture life 2684.4 h), visual inspection revealed what appeared to be a crack very near the fusion line.

The three long-time tests, on the other hand, failed with a flat fracture, and the failure was very near the fusion line (Fig. 10). We could not determine visually how near the failure was to the fusion line. Examination of the fracture surface with a low-magnification stereo microscope (<10×) revealed that in places the weld bead structure was visible, thus indicating a proximity to the fusion line.

One 2 1/4 Cr-1 Mo steel base metal test was conducted at 172 MPa on a specimen that was postweld heat treated 1 h at 732°C and aged 2000 h at 566°C. This creep curve differed little from that of the composite specimen (Fig. 11). The composite specimen failed in 698.3 h, the base metal specimen failed in 704.5 h. Likewise, the minimum creep rates

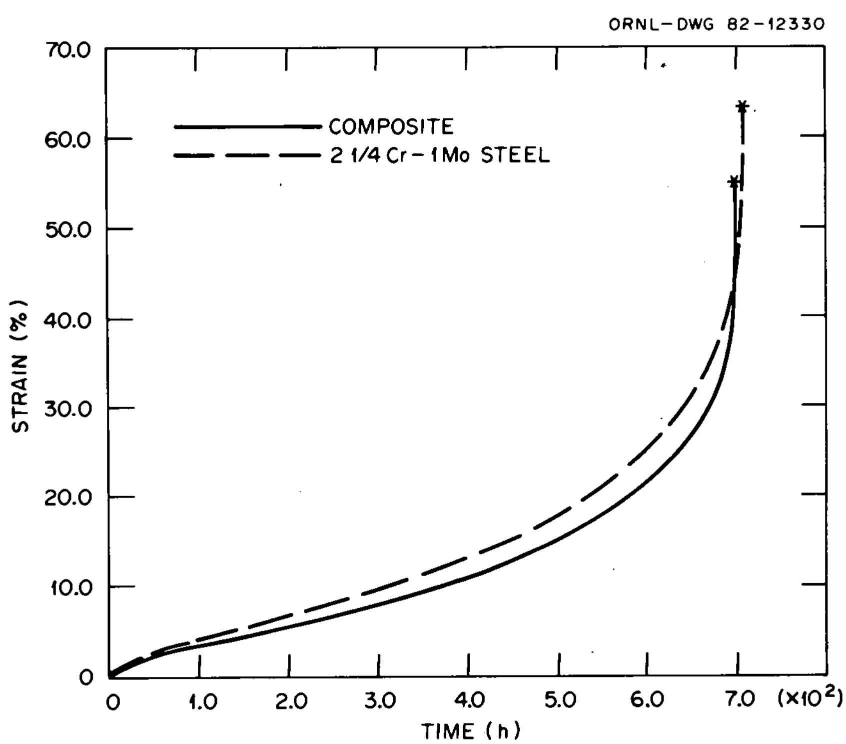

Fig. 11. A comparison of the creep curves for 2 1/4 Cr-1 Mo steel base metal and composite weldment specimens tested at 172 MPa at 510°C.

agreed reasonably well (0.0269%/h for the base metal, 0.0201%/h for the composite specimen; note that the latter value assumes that deformation occurred over only the 2 1/4 Cr-1 Mo steel portion of the gage section). Similar comparisons were obtained for two other base-metal tests. Thus, all indications are that for the high-stress tests on composite specimens, most of the deformation occurs within the 2 1/4 Cr-1 Mo steel and the deformation is little different from an all-base-metal specimen. Only for long-time (low-stress) tests does the weld metal play a role in the failure. No low-stress base-metal tests were made.

At 593°C (Table 7), there were too few tests to determine the extent of curvature on the creep-rupture curves, although a definite downward curvature was evident (Fig. 12). The test atmosphere (air or flowing argon) had little effect on the results, either on the rupture life (Fig. 12) or the creep strain-time behavior (Fig. 13). However, as discussed in the following section, the argon contained considerable oxygen.

At 593°C, only the highest stressed tests (97 MPa) failed in the 2 1/4 Cr-1 Mo steel at a large distance from the fusion line and with considerable plastic deformation. The specimens tested at 83 and 69 MPa failed adjacent to the fusion line. These specimens displayed much less plastic deformation (smaller reduction of area and elongation, Table 7).

Table 7. Creep-rupture properties of composite 2 1/4 Cr-1 Mo/ERNiCr-3/alloy 800H specimens at 593°C

Stress (MPa)	Rupture time (h)	Total elongation (%)	Reduction of area (%)	Minimum creep rate (%/h)
		Air tests		
97	655.7	24.7	91.4	0.00728
83	3025.9	8.4	33.6	0.000905
69	7265.0	2.5	28.4	0.000131
		Argon tests		
97	726.7	22.6	90.4	0.00440
83	2731.1	7.0	28.4	0.00101
69	5625.2	2.5	19.9	0.000133

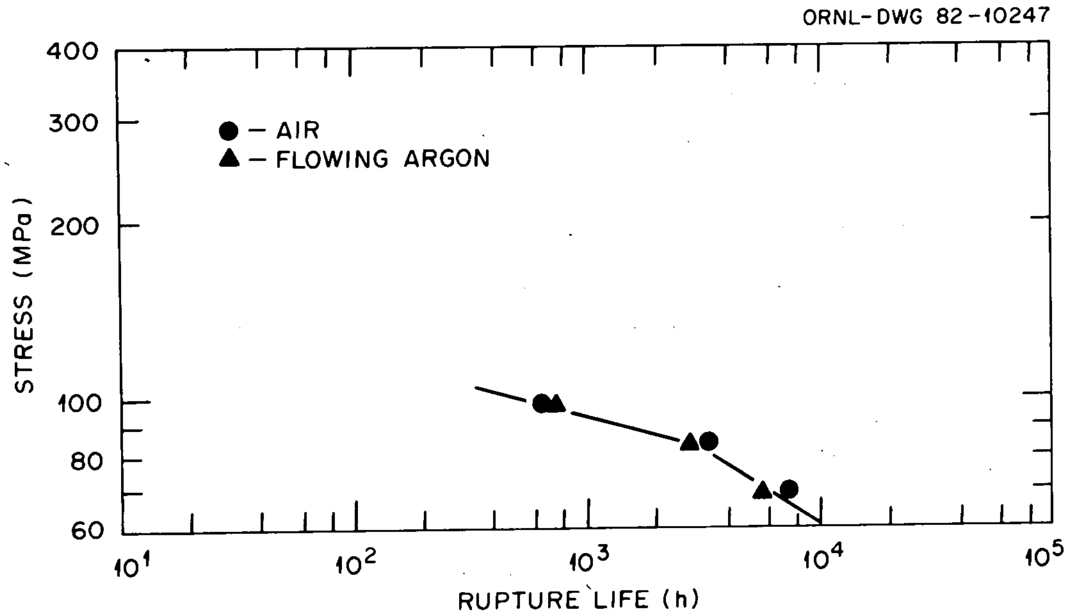

Fig. 12. Stress-rupture curve at 593°C for composite weldment specimens taken from prototypic pipe weld.

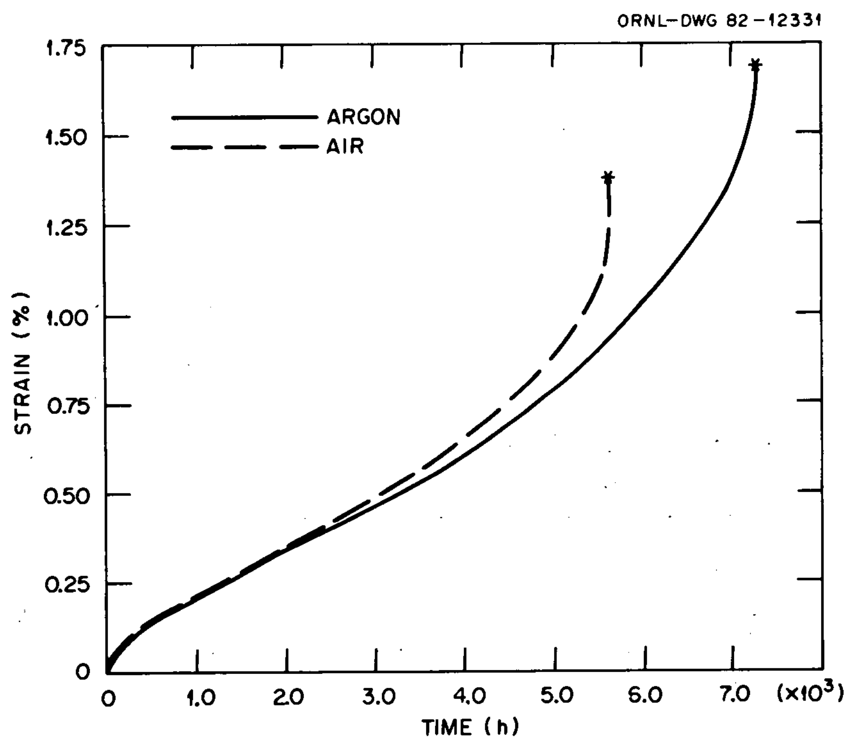

Fig. 13. Comparison of creep curves for composite weldment specimens tested in air and flowing argon at 83 MPa and 593°C.

METALLOGRAPHIC OBSERVATIONS

The alloy 800H base metal and the ERNiCr-3 weld metal were typical for these alloys (Fig. 14). Because these materials were not involved in the fracture, they will not be further discussed. The isothermally annealed 2 1/4 Cr-1 Mo steel base metal well back from the fusion line was a polygonal ferrite-bainite microstructure, which is typical for this heat-treated condition [Fig. 15(a)].

As shown in Fig. 15(b), the welding process causes a variation in the microstructure of the 2 1/4 Cr-1 Mo steel near the weld fusion line (this part of the discussion addresses only the 2 1/4 Cr-1 Mo steel that is not affected by diffusion to or from the weld metal). The 2 1/4 Cr-1 Mo steel is entirely bainite where it transforms to austenite from the heat of welding and rapidly cools after welding (i.e., in the region adjacent to the fusion line, where the steel is heated above the A_{c_3} temperature). Back from the fusion line, the microstructure varies from entirely bainite to a region of bainite and polygonal ferrite (where the steel was heated above the A_{c_1} but not the A_{c_3}). The relative amount of ferrite increases to the point where the temperature equaled A_{c_1}. Beyond this distance, the only effect of welding is the tempering of the 2 1/4 Cr-1 Mo steel base metal.

The low-ductility dissimilar-metal weld failures of interest occurred immediately adjacent to the fusion line in the region that involves metallurgical interaction between the 2 1/4 Cr-1 Mo steel base metal and the ERNiCr-3 weld metal.[1–8] The nature and origin of the microstructure immediately adjacent to the fusion line has been investigated in detail, as has its relationship to the fracture.[1–8] We will briefly discuss the microstructure at the fusion line in the following section. In this section we will discuss our metallographic observations on the fractures.

As stated in the previous section, visual observations indicated that fractures at 510°C for all but the three long-time tests (>7000 h) occurred by a ductile cup-cone mode. This was verified by metallographic

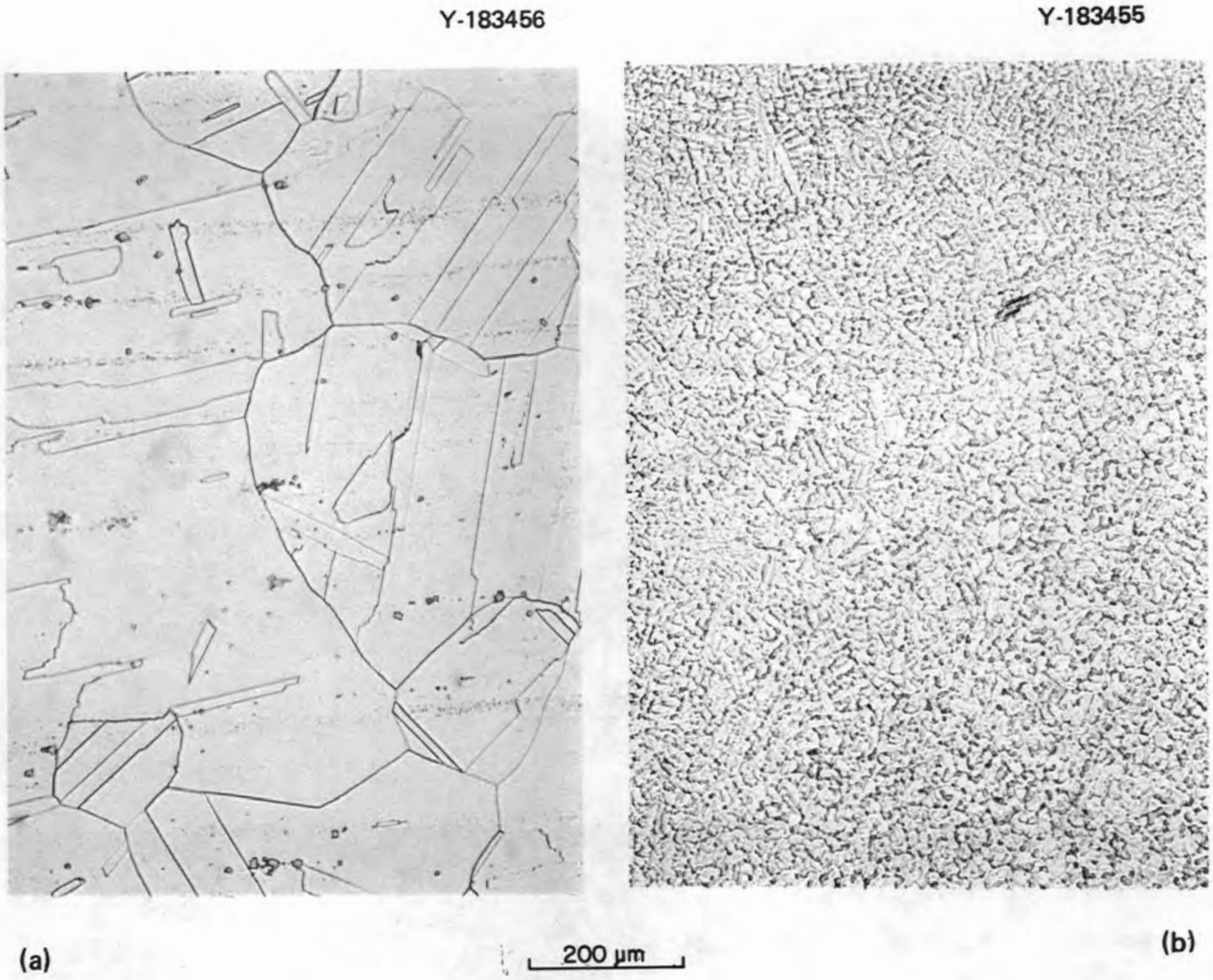

Fig. 14. Microstructure of (a) alloy 800H base metal and (b) ERNiCr-3 weld metal of the composite weldment.

Y-183454

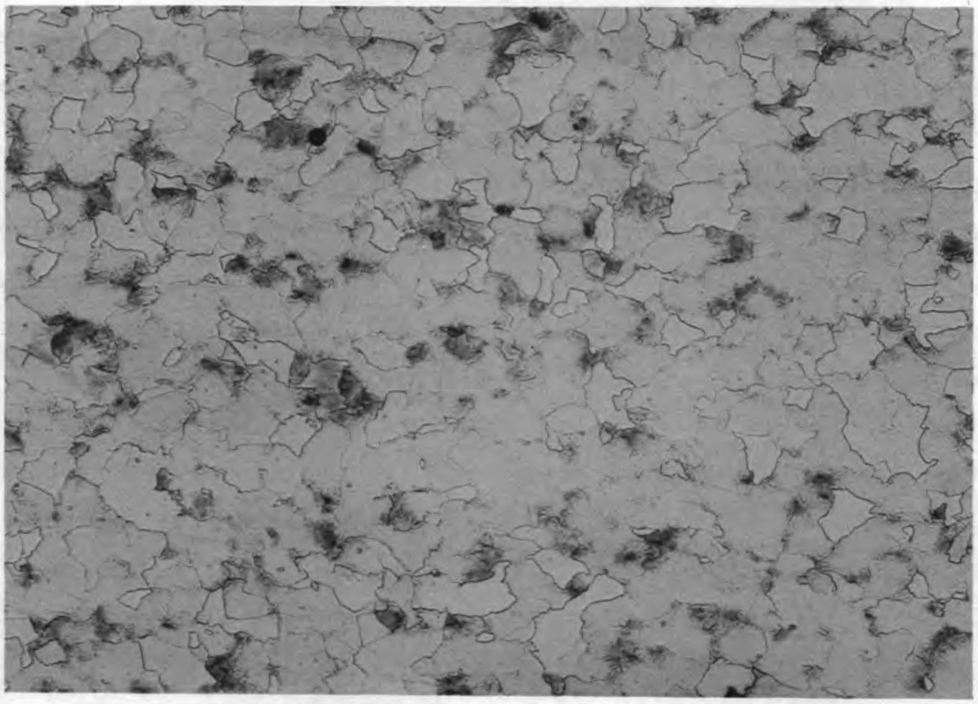

(a) 200 μm

Y-183452

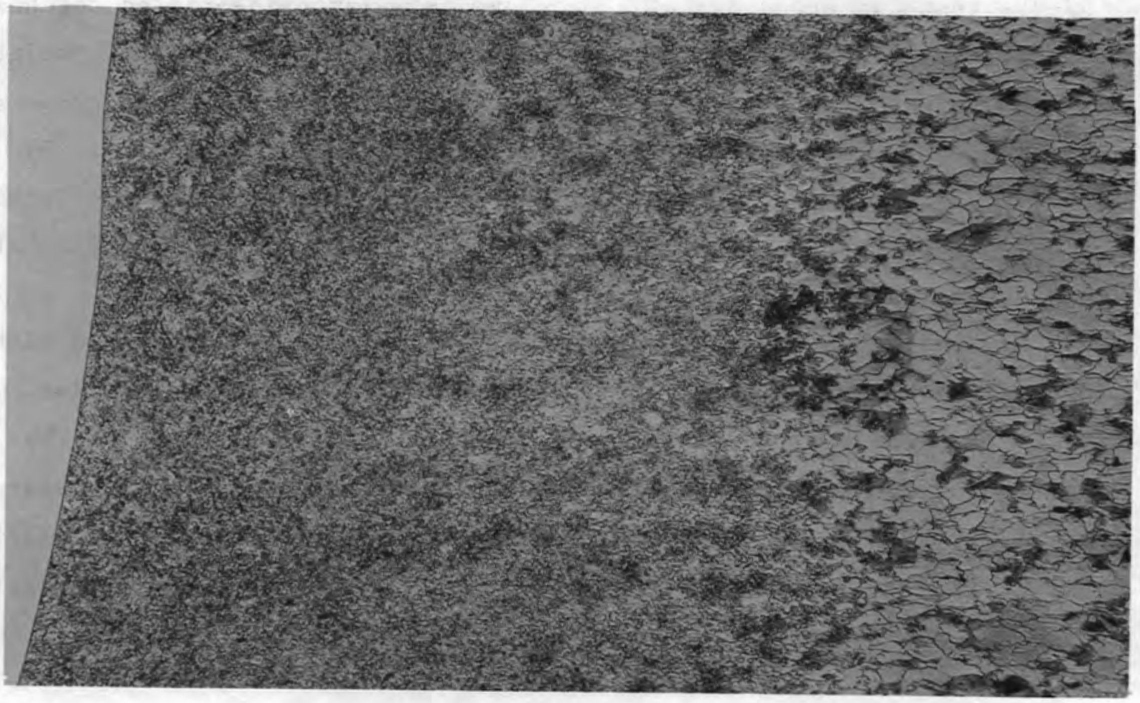

(b) 400 μm

Fig. 15. Microstructure of 2 1/4 Cr-1 Mo steel. (a) Base metal unaffected by welding. (b) The variation in microstructure in going from the fusion line (near left) to the unaffected base metal (right).

observation. The fractures were typical of those for 2 1/4 Cr-1 Mo steel base metal tested under similar conditions.[16] Although the fracture for these specimens occurred well away from the fusion line, the microstructure at the fusion line was affected, the effect changing with stress (or time of exposure at elevated temperature). For the specimens examined, an oxide-filled notch or crack was inevitably present in the 2 1/4 Cr-1 Mo steel very near the fusion line (Figs. 16–18). In some instances, quite a small oxide notch was observed [Fig. 16(a)], whereas other specimens contained an oxide-filled crack of considerable length [Fig. 16(b)]. The extent of the crack or notch depended somewhat on stress (or time in test), although a notch was present after even the shortest creep-rupture times [Fig. 16(a)]. We noted in the previous section that the evidence of a crack could be detected visually on one of the lowest stress test specimens that failed transgranularly. The cracks were always filled with oxide that formed from the 2 1/4 Cr-1 Mo steel. The relationship of the oxide to the 2 1/4 Cr-1 Mo steel and the ERNiCr-3 weld metal is shown in Fig. 17.

The two tests that failed in a ductile-transgranular mode at 593°C (97-MPa tests in argon and air) displayed similar oxide-filled notches or cracks (Fig. 18). When the amounts of oxide that formed within the cracks and on the external surface of the specimen that was tested in argon are compared with those formed under similar conditions in air (Fig. 19), it is obvious that the argon test cannot be assumed to have been conducted in an inert atmosphere. A new inert-gas test system will be required before such creep tests can be conducted.

For the three long-time rupture tests at 510°C, which failed with very little deformation, failure occurred very near the fusion line (Fig. 20). These fractures obviously occurred by propagation of the interface notch or crack observed on the specimens that failed transgranularly (Figs. 16–18). Similar observations were made on the specimens tested at 593°C at 83 and 69 MPa (Fig. 21). These specimens also failed with limited amounts of deformation (Table 7).

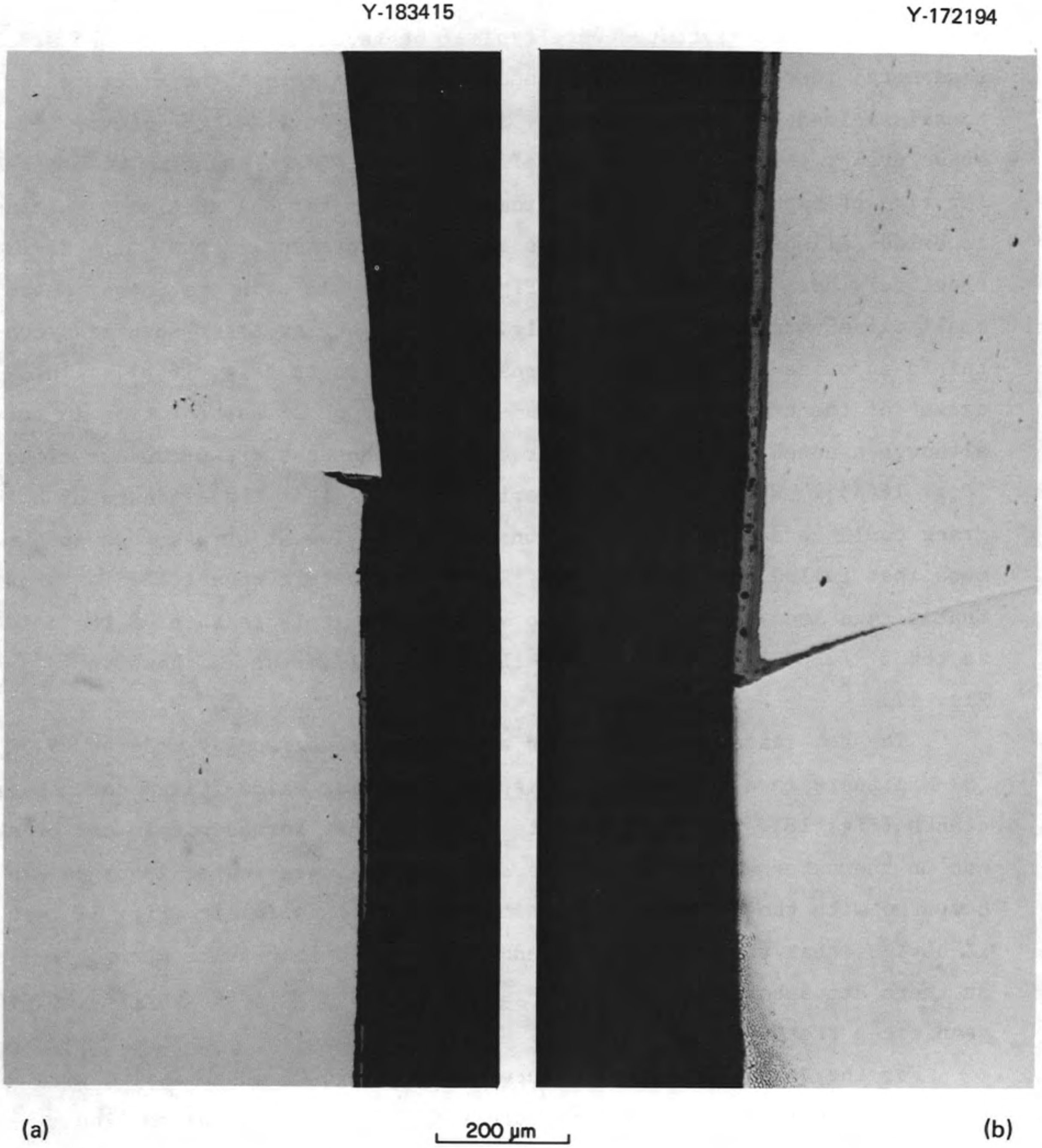

Fig. 16. Example of oxide notch or crack that formed on stress-rupture specimens that were tested at 510°C and failed in a ductile manner in the 2 1/4 Cr-1 Mo steel base metal. (a) Rupture life 146.9 h. (b) Rupture life 1313.7 h.

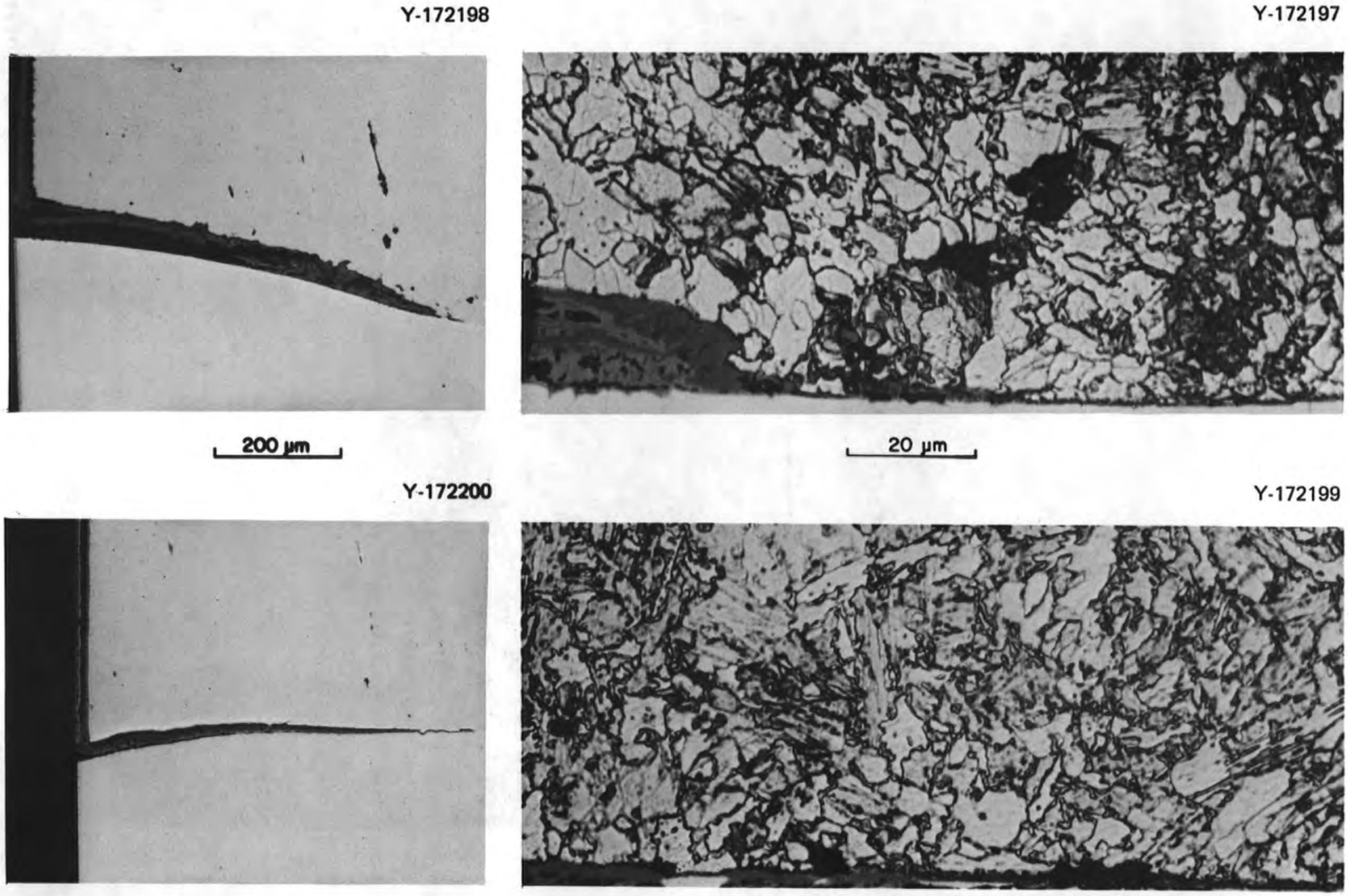

Fig. 17. Examples of oxide-filled cracks and relation to the fusion line on stress-rupture specimens tested at 510°C. Top: rupture life 1508.4 h. Bottom: rupture life 809.2 h.

Y-179661

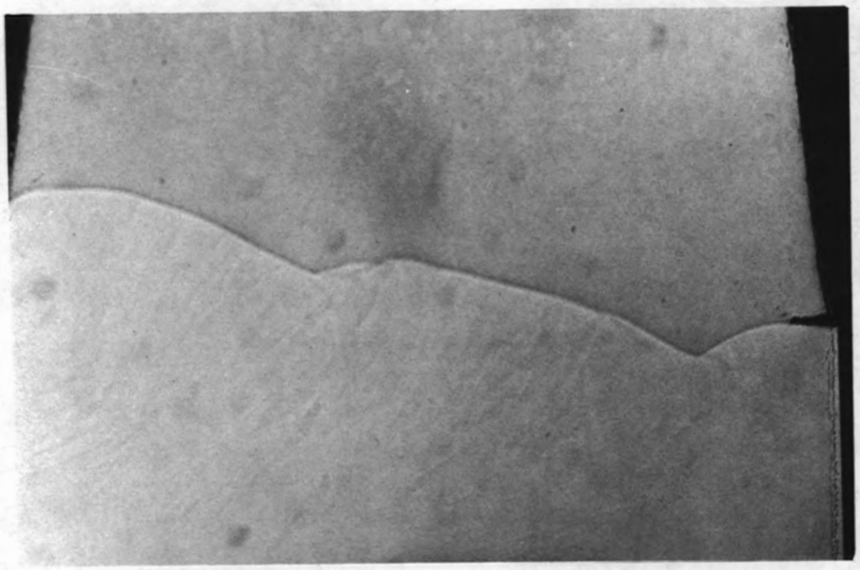

Y-179674

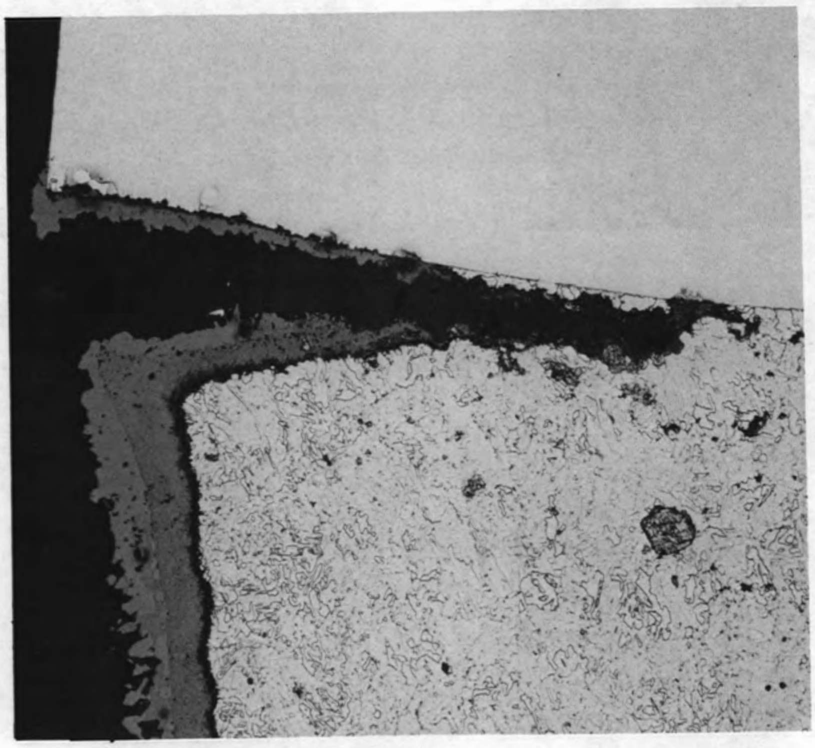

Fig. 18. Example of oxide notch or crack on specimen from prototypic pipe weld tested at 593°C in argon. Rupture life: 726.6 h.

Y-179676 Y-179675

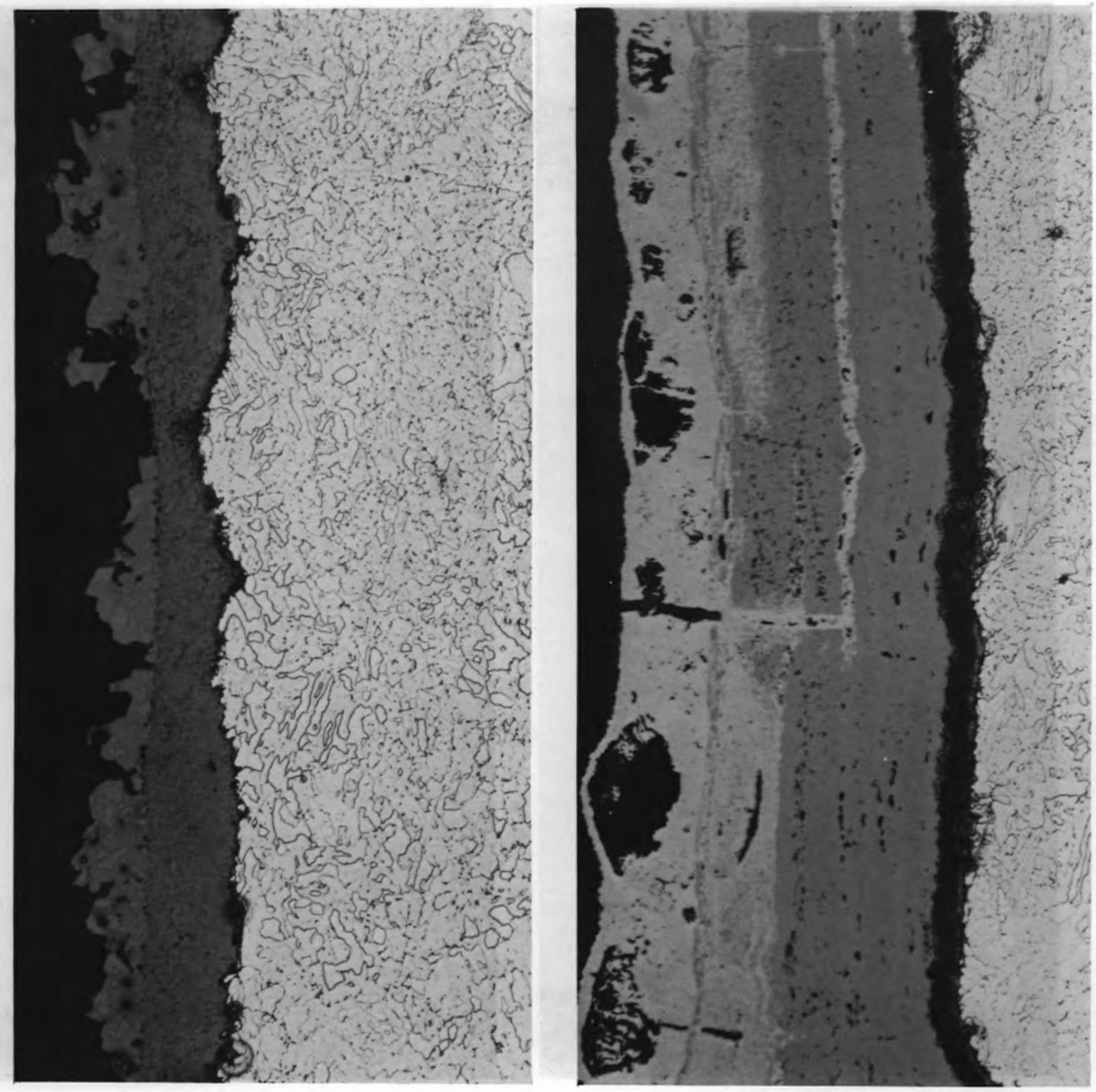

(a) 40 µm (b) 40 µm

Fig. 19. A comparison of the oxide scales formed at 593°C in (a) flowing argon and (b) air.

Y-175438 Y-175439

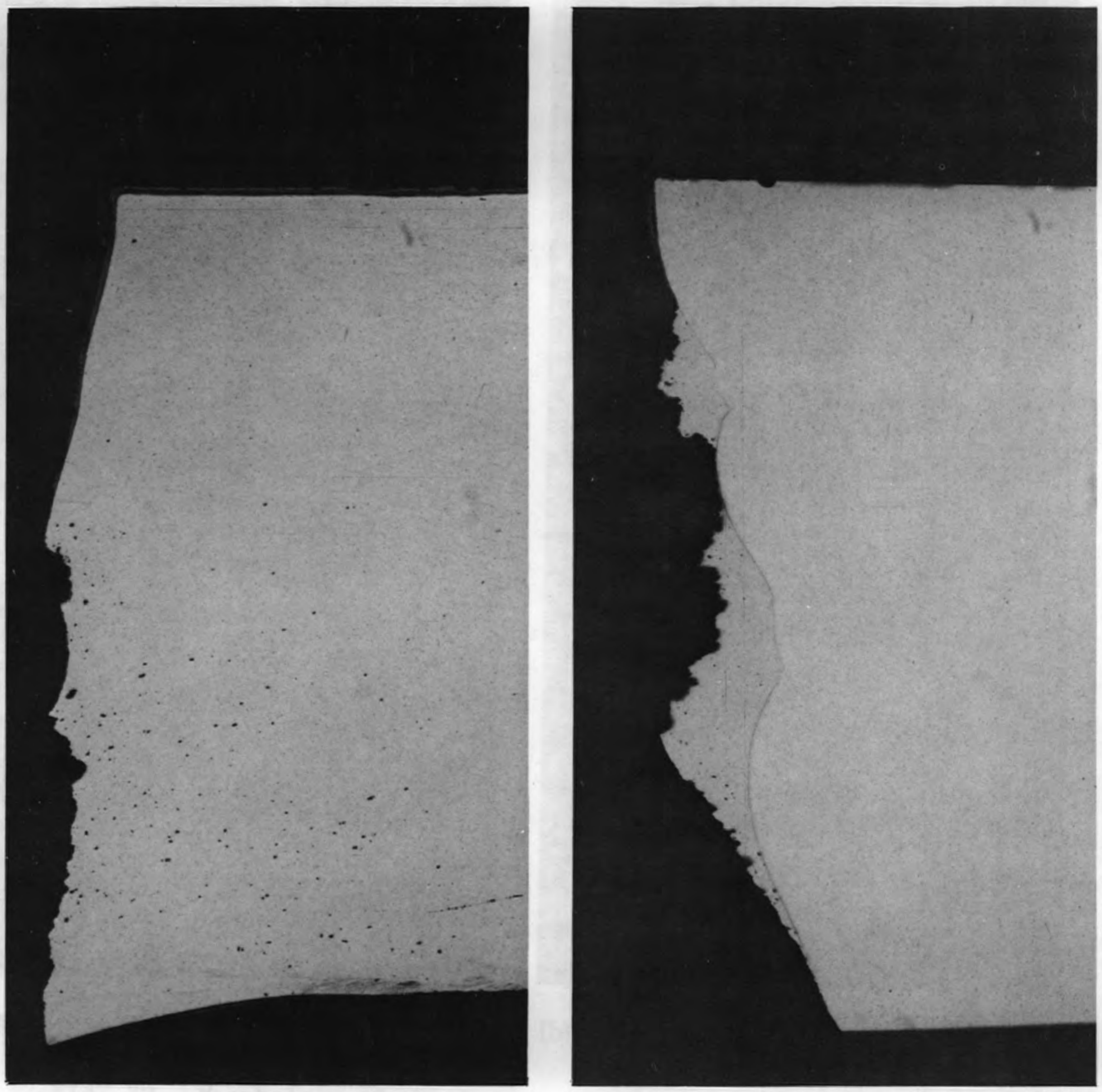

(a) 1000 mm (b) 1000 mm

Fig. 20. Morphology of the interface fracture of the composite specimen postweld heat treated 1 h at 732°C, aged 1000 h at 510°C, and tested at 131 MPa at 510°C (rupture life 8768.4 h). Unetched. (a) 2 1/4 Cr-1 Mo steel. (b) ERNiCR-3 with adhering 2 1/4 Cr-1 Mo steel.

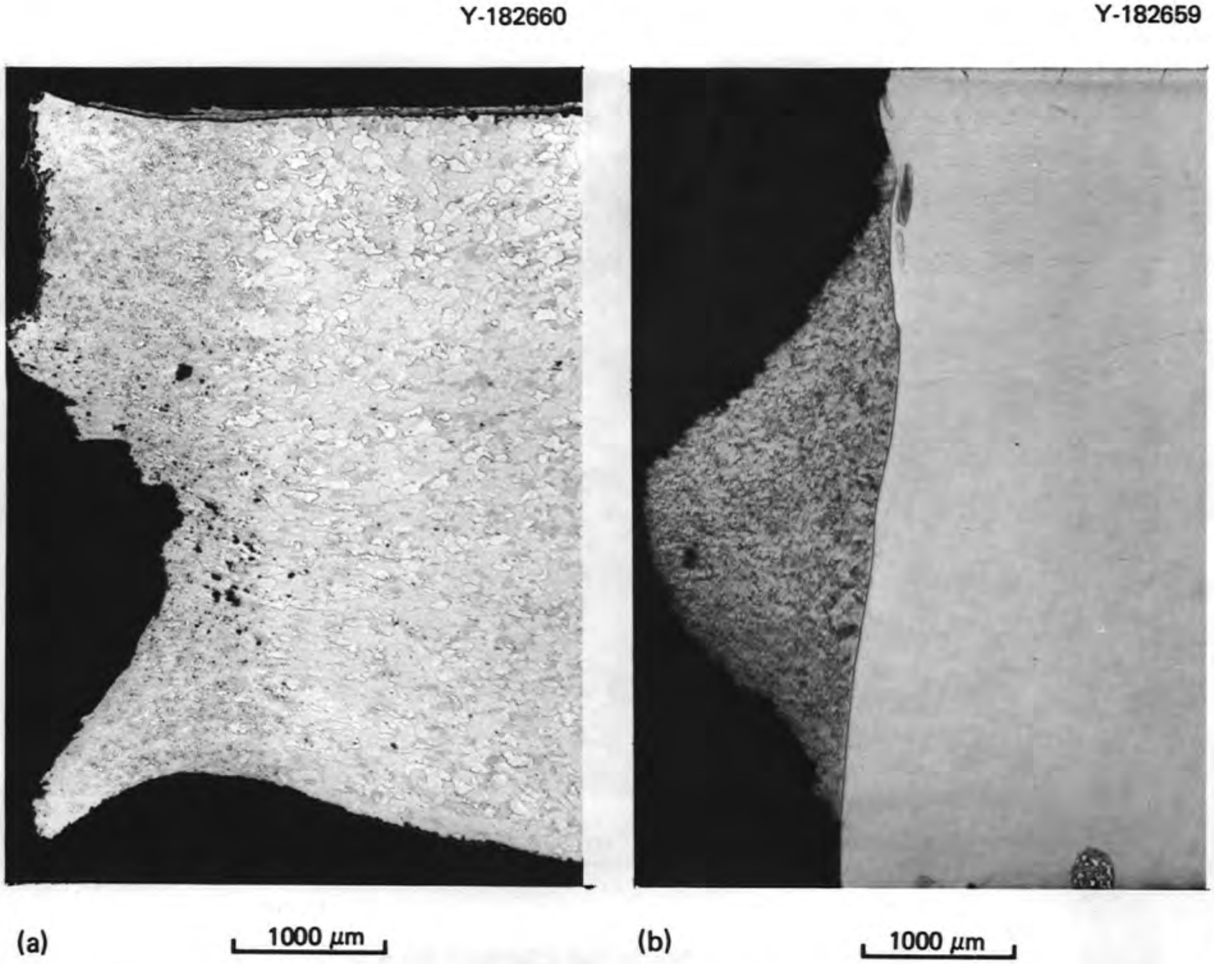

Fig. 21. Etched interface microstructure of creep-rupture specimen from prototypic pipe weld tested in air at 83 MPa at 593°C. (a) 2 1/4 Cr-1 Mo steel. (b) ERNiCr-3 weld metal with adhering base metal.

Before the low-stress tests were sectioned for metallography, the fracture surfaces were examined by scanning electron microscopy (SEM). Two morphologically distinct regions could be detected. A flat region was immediately adjacent to the external surface; this region surrounded a region that was quite rough [Fig. 22(a)]. Both regions were quite highly oxidized. However, at high magnification, the roughened center portion was found to be dimpled, as is typical of a ductile fracture [Fig. 22(b)].

The SEM observations are easily correlated with the optical microscopy. Immediately adjacent to the external surface, the fracture is very flat and essentially parallel to the fusion line. As discussed

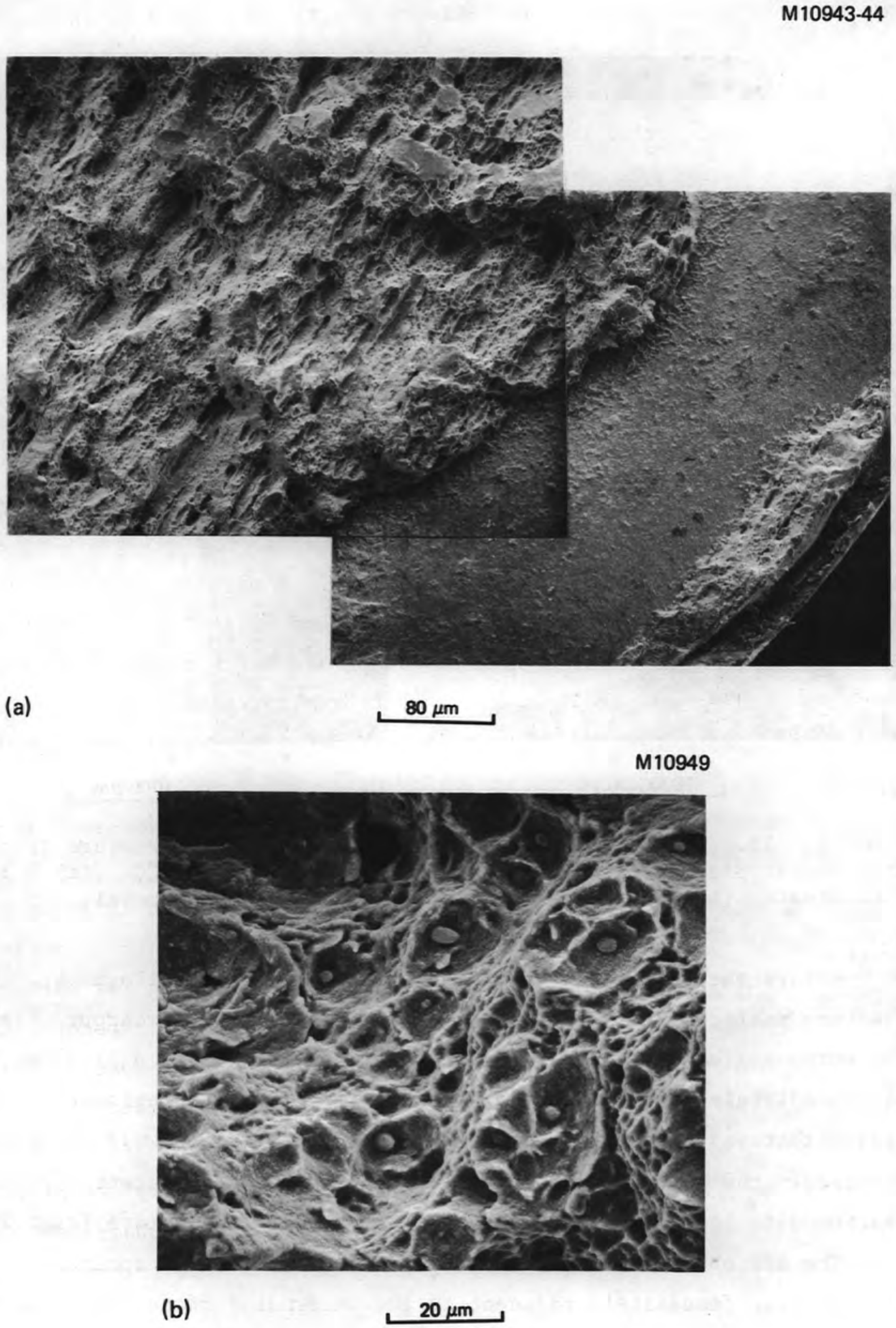

Fig. 22. Scanning electron micrograph of ERNiCR-3 fracture surface of composite specimen with 1-h PWHT at 732°C tested at 134 MPa at 510°C (rupture life 7823.4 h). (a) Low magnification showing different fracture morphologies. (b) High magnification of center portion of fracture.

below, this is an intergranular fracture. Further into the specimen the fracture deviates from the fusion line and appears to be quite ductile (Figs. 20 and 21). The fracture apparently started as a notch at the external surface, then developed into a crack and propagated along grain boundaries toward the center of the specimen. After the grain boundary crack has propagated some distance into the specimen, the loss in load-bearing cross section causes the true stress to increase until the fracture begins to propagate in a ductile-transgranular mode (similar to the high-stress tests). Note the holes in the center of the 2 1/4 Cr-1 Mo steel portion of the fractured specimens [Figs. 20(a) and 21(a)]. These are typical of a ductile-transgranular fracture.

Although the fracture surfaces of the specimens are covered with oxide, there are indications that the crack did not propagate on the fusion line, but rather propagated on 2 1/4 Cr-1 Mo steel grain boundaries approximately one grain width from the fusion line (<10 μm from the fusion line) (Fig. 23). Many small islands of 2 1/4 Cr-1 Mo steel on the ERNiCr-3 weld metal were found (Fig. 23). The thick oxide layers that are observed on the ERNiCr-3 weld metal that does not contain these islands must have formed from the islands of 2 1/4 Cr-1 Mo steel left behind. It is highly improbable that such a thick oxide layer would form on the ERNiCr-3 surface, since there is almost no oxide on the external surface of this oxidation-resistant alloy.

Some investigators have reported creep-induced voids in grain boundaries parallel to the fusion line.[7] It is implied that these voids lead to the failure. We examined our metallographic specimens for such voids but were unable to detect any. In addition to optical microscopy, these observations included SEM studies (to 10,000×) on the 69- and 87-MPa tests at 593°C (the higher temperature should favor cavity formation). These specimens were studied in the center region, where the 2 1/4 Cr-1 Mo steel adhered to the weld metal. If creep cavities formed, they should still be present in this region after failure. No cavities were observed. On the other hand, if cavities form only slightly ahead of the transgranular crack, oxidation would obliterate evidence of them.

Y-173482

40 μm

Y-175520

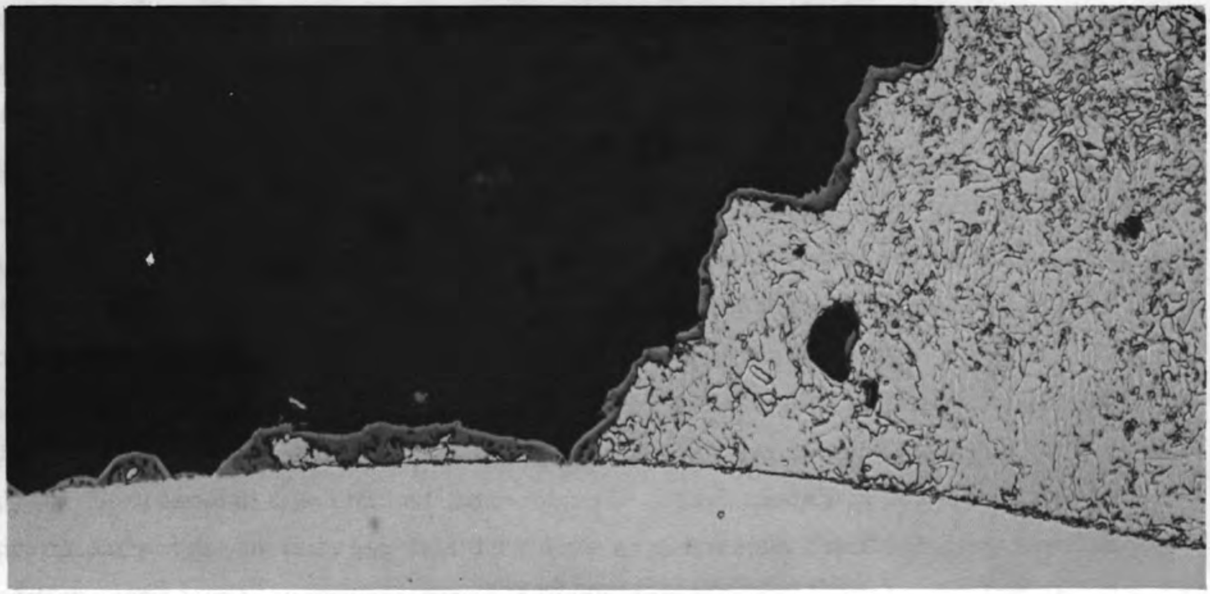

40 μm

Fig. 23. Microstructure near the region where the fracture mode changes from brittle to ductile, illustrating how the brittle fracture proceeds along grain boundaries approximately one small grain into the 2 1/4 Cr-1 Mo steel. In some cases these small grains have been subsequently consumed by oxide. Specimen is the same as Fig. 22.

DISCUSSION

Dissimilar-metal weld joints between an austenitic stainless steel and a ferritic steel (primarily 2 1/4 Cr-1 Mo steel) in fossil-fired steam plants operating near 560°C tend to fail under operating conditions that involve temperature cycling. Failures occur in the 2 1/4 Cr-1 Mo steel very near the fusion line (15–25 μm).[8] In creep-rupture tests on weldment specimens taken from a 2 1/4 Cr-1 Mo steel/ERNiCr-3 weld metal/alloy 800H dissimilar-metal weldment, we produced fractures in the 2 1/4 Cr-1 Mo steel near the fusion line, similar to the fractures that occur in operating fossil-fired steam plants. No thermal cycles were necessary to produce these failures; thermal cycles are necessary in the fossil-fired plants.

As was true in previous tests,[7] such fractures occurred only for creep-rupture tests at quite low stresses (long rupture lifetimes); this was especially true at 510°C. At high stresses, the rate of crack propagation at the interface is slow relative to creep of the 2 1/4 Cr-1 Mo steel. Under these conditions, a transgranular failure results in the 2 1/4 Cr-1 Mo steel. Only at low stresses is it possible to propagate an interface crack, although even in this case much of the fracture is ductile transgranular. However, because the initial portion of the failure occurred by a crack propagating along the interface, the ductile portion of the fracture is also restricted to the vicinity of the interface, thus resulting in a small measured total elongation and reduction of area.

The metallographic observations on the failed creep-rupture specimens agree with our proposed failure mechanism,[8] which was summarized in the Introduction. That mechanism postulated a depletion of chromium in the 2 1/4 Cr-1 Mo steel matrix adjacent to the weld metal interface. This chromium was assumed to be incorporated in precipitates that form in grain boundaries parallel to the fusion line. The loss of matrix chromium during welding, postweld heat treatment, and service lowers oxidation resistance. This leads to an oxide notch in the low-chromium region and eventually to an oxide-filled crack that propagates under the action of the imposed stress. In our previous paper we postulated a fatigue crack, whereas in the present tests the crack forms under the action of a constant load (creep crack). The fatigue fracture was proposed for operating fossil-fired plants because of the cyclic thermal stresses present in those plants.[8] Regardless of whether a fatigue or creep stress operates on the crack, the reason for the crack is always the chromium depletion.

All the metallurgical elements that were present in the microstructures of the small tubes taken from the fossil-fired plants appear to be present in the welds of this study. However, everything is on a finer scale. A very narrow dark region appears to be almost on the fusion line (Fig. 24). This is probably the "dark-etching phase" that has been identified as tempered martensite.[8,17–20] Fracture occurs by a crack propagating in grain boundaries parallel to the fusion line — closer to the fusion line than the crack in the tubes previously examined.[8]

The finer scale of microstructure is undoubtedly a reflection of the difference in the geometry of the weldment used in this study. The fossil-fired transition joints were made in 25.4-mm-diam by 12.7-mm-thick tubing, whereas the present welds were made in 19-mm-thick plates, thus giving rise to different cooling rates and, thus, different microstructures.

Because of the fineness of the microstructure of the 2 1/4 Cr-1 Mo steel in the vicinity of the fusion line, it is difficult to detect any precipitates in the grain boundaries in this region, as was possible for the tubes.[8] It is also difficult to determine the path of the crack. Cracks usually propagated about one grain width back from the fusion line, which also agrees with previous observations[8] (Fig. 23).

The proximity of the crack to the fusion line is the reason the oxide appears to have formed on the weld metal. That is, the amount of high-iron, low-chromium material left on the weld metal is small, and in some cases essentially all of it is consumed as oxide by the time the creep test is completed.

Although there has been some discussion about the possibility that dissimilar-joint failures can begin inside the 2 1/4 Cr-1 Mo steel and not at the external surface,[21] the creep-rupture fractures of this study are definitely nucleated at the external surface. All indications are that the cracks are nucleated at the oxide notch. The fact that no creep cavities were observed does not mean that they may not form, although the

Y-182319

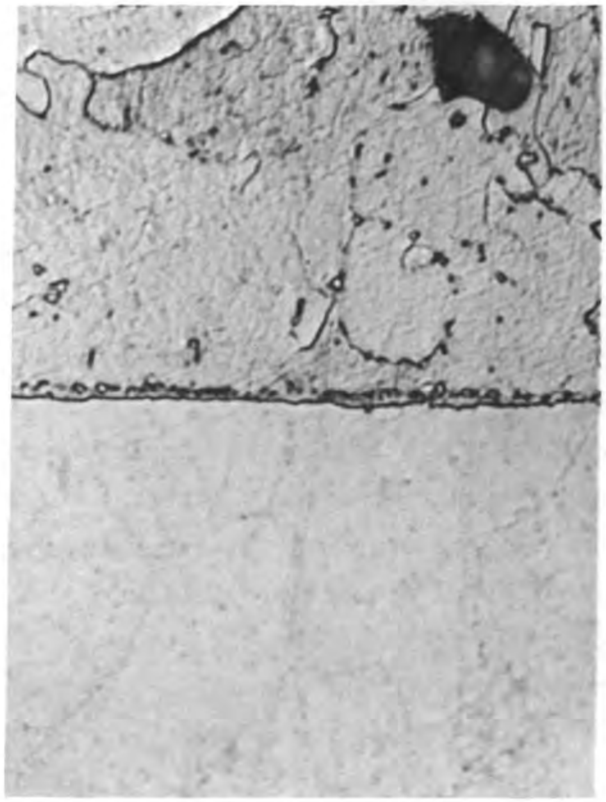

Fig. 24. High-magnification of weld interface showing what appears to be a row of precipitate particles parallel to the fusion line.

postulated failure mechanism does not require their presence. However, if present, they could speed crack propagation. (Only a few observations of creep cavitiation in the 2 1/4 Cr-1 Mo steel have been made.[7]) Cavities might be expected after long times at 593°C but are less likely at 510°C. Since none were observed at 593°C and quite large cracks formed at 510°C within 1000 h, creep cavitation is apparently not necessary for an interface failure of the type observed in this study.

Our microstructural observations are similar to those made in the General Electric Transition Joint Life Tests (TLJT) on the large test specimen shown in Fig. 3.[13,14,22] In those tests the specimens were tested under severe temperature-transient conditions: the pipe specimen was heated to 593°C and then cooled at rates as high as 11.2°C/s. Failure occurred in as few as 20 cycles.

Failure occurred very near the interface between the ERNiCr-3 and the 2 1/4 Cr-1 Mo steel, and the crack "originated at or very close to the outside surface of the weld joint."[22] When the test was continued until the pipe separated, the crack propagated very near the interface through over 50% of the wall thickness; then it propagated rapidly through the 2 1/4 Cr-1 Mo steel — a ductile failure caused by the increase in true stress due to the reduction of load-carrying wall. Also, all major cracks contained oxide "at the outside surface and well down into the crack." And, "where the cracks were open, oxide was found all the way down to what appeared to be the crack tip."[22]

The observations on the TLJT agree completely with the metallographic observations on the creep tests at low stresses. Likewise, the observations are in line with the proposed failure mechanism.

With the exception of the higher yield strength and ultimate tensile strength and longer rupture life for the weldment specimen given the 1-h PWHT at 732°C, the effect of PWHT and aging were generally as expected. The only apparent exception was the observation on the long-time (>7000 h) creep failures. The three specimens tested at the low stresses differed very little in strength (Fig. 10), regardless of whether the specimen was aged or not, even though the joint aged 2000 h at 566°C was considerably weaker than the other materials at higher stresses (short rupture times). Furthermore, although the low-stress specimen of that joint ruptured after more than 9500 h (longer than the other specimens), it had a reduction of area almost twice that of the other two low-stress specimens. It has been assumed that thermal aging increases the tendency toward low-ductility, interface-type fractures.[1-6,11]

The observation of interface-type failures on welds made between 2 1/4 Cr-1 Mo steel and alloy 800H does not have any implications on the reliability of a transition joint in a fast breeder reactor. The failure occurs at the 2 1/4 Cr-1 Mo steel/ERNiCr-3 weld metal interface; a similar failure would be expected for a test where 2 1/4 Cr-1 Mo steel is joined directly to type 316 stainless steel. It is in the operating transition joint that differences would be noted for the two types of joint. Under operating conditions during service, the stresses on the joint are thermal stresses during startup and shutdown; these stresses are generated by differences in thermal expansion coefficients for the various joint component materials. The thermal stress developed on a joint with an alloy 800H spool piece should be smaller than that developed on a joint without a spool piece. Thus, the joint with a spool piece will be less likely to fail under similar operating conditions.

SUMMARY AND CONCLUSIONS

Tensile and creep-rupture tests were conducted on dissimilar-metal weld joints made between 19-mm-thick plates of 2 1/4 Cr-1 Mo steel and alloy 800H with hot-wire ERNiCr-3 filler metal. Tests were made on composite specimens taken from these weldments after they had received nine different PWHT and aging conditions: (1) those given PWHTs of 1 h at 677°C, 1 h at 732°C, and 10 h at 732°C; (2) specimens given the same PWHTs, then aged 1000 h at 510°C; (3) specimens given the same PWHTs and aged 2000 h at 566°C.

The tensile tests were made at room temperature, 510, and 566°C; base metal tensile properties for each component of the weldment were determined under similar conditions. Creep-rupture tests were made on composite specimens at 510°C. In addition, tensile tests were made at room temperature and 593°C and creep-rupture tests were made at 593°C in support of the Transition Joint Life Test being conducted by General Electric. Specimens for these tests were taken from a 2 1/4 Cr-1 Mo steel/ERNiCr-3/alloy 800H joint that was made in an 0.46-m-diam pipe. This joint is prototypic of the joints in the CRBRP. Identical creep-rupture tests at three stresses at 593°C were made in air and flowing argon.

The following summarizes the observations and conclusions from these tests.

1. All tensile tests failed in a ductile-transgranular mode in the 2 1/4 Cr-1 Mo steel base metal well away from the fusion line. Such a fracture was expected in light of the base metal properties for the three components of the composite specimens.

2. Creep-rupture fractures for the plate-weldment specimens that ruptured at 510°C in 2000 h or less occurred in the 2 1/4 Cr-1 Mo steel by a ductile-transgranular mode. Failures for three specimens that ruptured in greater than 7000 h occurred with very little ductility in the 2 1/4 Cr-1 Mo steel very near the fusion line.

3. Creep-rupture fractures at 593°C were similar to those at 510°C: short-time (<800 h) failures were ductile, long-time (>3000 h) failures displayed little ductility and occurred near the fusion line. Although the tests in argon showed similar behavior to those in air, the "inert atmosphere system" used for the argon tests contained too much oxygen to allow these tests to be classified as actual inert-atmosphere tests.

4. Metallographic observations revealed that the low-ductility interface fractures occurred just inside the 2 1/4 Cr-1 Mo steel less than about 10 μm from the fusion line.

5. The metallographic observations on the ductile and low-ductility creep-rupture fractures showed that a crack nucleated below an oxide notch at the external surface. The oxide notch forms because chromium is depleted in the matrix by carbide formation in grain boundaries that are parallel to the fusion line. This low-chromium matrix region is a region of low oxidation resistance (oxidation resistance depends on the matrix chromium concentration). Preferential oxidation of the low-oxidation-resistant region adjacent to the grain boundary leads to an oxide notch and an oxide-filled crack that propagates essentially transgranularly toward the center of the specimen cross section. The mechanism agrees with that previously postulated for the failure of dissimilar-metal weld joints in fossil-fired steam plants.

ACKNOWLEDGMENTS

Special thanks are due to several people. J. L. Griffith carried out the experimental work. C. W. Houck did the metallography. The manuscript was reviewed by R. W. Swindeman and J. P. Strizak. Sig Peterson edited the manuscript and D. L. LeComte prepared the final copy.

REFERENCES

1. R. V. Blaser, F. Eberle, and J. T. Tucker, "Welds Between Dissimilar Alloys and Full Size Steam Piping," *Am. Soc. Test. Mater. Proc.* 50, 789–807 (1950).

2. G. E. Lien, F. Eberle, and R. D. Wylie, "Results of Service Test Program on Transition Welds Between Austenitic and Ferritic Steels at the Phillip Sporn and Twin Branch Plants," *Trans. ASME* 76, 1075–83 (1954).

3. R. W. Emerson, R. W. Jackson, and C. A. Dauber, "Transition Joints Between Austenitic and Ferritic Steel Piping for High Temperature Steam Service," *Weld. J. (N.Y.)* 41, 385-s–393-s (1962).

4. J. T. Tucker and F. Eberle, "Development of a Ferritic-Austenitic Weld Joint for Steam Plant Applications," *Weld J. (N.Y.)* 35, 529-s-40-s (1956).

5. J. Barford and K. S. Probert, "Interfacial Effects in Dissimilar Steel Joints," paper presented at the International Conference on Welding Research Related to Power Plants, Marchwood Engineering Laboratories, Sept. 17–21, 1972.

6. R. J. Gray, J. F. King, J. M. Leitnaker, and G. M. Slaughter, *Examination of a Failed Transition Weld Joint and the Associated Base Metals*, ORNL-5223, January 1977.

7. R. D. Nicholson, *The Creep Rupture Properties of Austenitic and Nickel-Based Transition Joints*, Central Electricity Generating Board, Marchwood Engineering Laboratories, England, RD/M/1176N81, June 1981.

8. R. L. Klueh and J. F. King, *Ferritic-Austenitic Transition Joint Failures*, ORNL-5637, April 1980.

9. W. R. Apblett, Jr., R. P. Dunphy, and W. S. Pellini, "Transformation of Cr-Mo Steels During Welding," *Weld. J. (N.Y.)* 33, 57-s–64-s (1954).

10. P. Doig and P.E.J. Flewitt, "Segregation of Chromium to Prior Austenite Boundaries During Quenching of 2 1/4 Cr-1 Mo Steel," *Acta Metall.* 29, 1831–41 (1981).

11. J. F. King, M. D. Sullivan, and G. M. Slaughter, "Development of an Improved Stainless Steel to Ferritic Steel Transition Joint," *Weld J. (Miami)* 56, 354-s–58-s (1977).

12. A. W. Dalcher, T. M. Yang, C. L. Chu, "High-Temperature Thermal-Elastic Analysis of Dissimilar Metal Transition Joints," *J. Eng. Mater. Technol.* 99, 65–69 (1977).

13. R. T. Hartle, H. J. Busboom, and P. J. Ring, *Transition Joint Welding Life Test Article Fabrication*, GEFR-00422, General Electric Co., San Jose, Calif., December 1978.

14. H. J. Busboom, T. M. Yang, and R. A. Day, "Transition Weld Development," pp. 74–83, *Program for the Development of Design Data LMFBR Steam Generator Materials*, GEFR-00067-4, General Electric Co., San Jose, Calif., July 1980.

15. R. L. Klueh and J. F. King, *Mechanical Properties of ERNiCr-3 Weld Metal Deposited by Gas Tungsten-Arc Process With Hot-Wire Filler Additions*, ORNL-5491, March 1979.

16. R. L. Klueh, *Effect of Postweld Heat Treatment on Creep and Creep-Rupture Properties of 2 1/4 Cr-1 Mo Steel*, ORNL-5751, June 1981.

17. N. F. Eaton and B. A. Glossop, "The Welding of Dissimilar Creep-Resisting Ferritic Steels," *Met. Constr. Br. Weld. J.* 1(12 suppl.), 6–10 (1969).

18. D. Wood, "Discussion Session 4, Welding Dissimilar Metals," *Met. Constr. Br. Weld. J.* 1(12 suppl.), 134–36 (1969).

19. J. Barford et al., "Weldment Cracking Involving a Complex Creep-Resistant Steel," pp. 54–65 in *Proc. Conf. Welding Creep-Resistant Steels*, The Welding Institute, Abington, England, 1970.

20. W.K.C. Jones, "Heat Treatment Effect on 2 Cr-Mo Joints Welded with a Nickel-Base Electrode," *Weld J. (Miami)* 53, 225-s–31-s (1974).

21. S. S. Long and F. V. Ellis, "Thermal Stress Analysis of Dissimilar Metal Welds," pp. 77–90 in *Properties of Steel Weldments for Elevated Temperature Pressure Containment Applications*, American Society for Mechanical Engineers, New York, 1978.

22. H. J. Busboom and P. J. Ring, "Progress Report on Transition Joint Life Test," *Fabrication Technology Program Ann. Progr. Rep. Sept. 30, 1981*, ORNL/MSP/1.4-81/1.

ORNL-5899
Distribution
Category UC-79Th,
-Tk, -Tr

INTERNAL DISTRIBUTION

1–2. Central Research Library
3. Document Reference Section
4–5. Laboratory Records Department
6. Laboratory Records, ORNL RC
7. ORNL Patent Section
8. C. R. Brinkman
9–13. F. R. Cox
14. J. A. Clinard
15. J. M. Corum
16. D. P. Edmonds
17. R. J. Gray
18. G. M. Goodwin
19. J. P. Hammond
20. R. F. Hibbs
21–25. J. F. King
26–31. R. L. Klueh
32. C. E. Pugh
33. G. M. Slaughter
34. R. W. Swindeman
35. J. P. Strizak
36. Alan Lawley (Consultant)
37. T. B. Massalski (Consultant)
38. R. H. Redwine (Consultant)
39. K. M. Zwilsky (Consultant)

EXTERNAL DISTRIBUTION

40–41. DOE, Office of Breeder Technology Projects, Washington, DC 20545
Director

42. DOE, Oak Ridge Operations Office, P. O. Box E, Oak Ridge, TN 37830
Office of Assistant Manager for Energy Research and Development

43–187 DOE, Technical Information Center, P. O. Box 62, Oak Ridge, TN 37830
For distribution as shown in TID-4500 Distribution Category:
UC-79Th (Structural Materials and Design Engineering)
UC-79Tk (Components)
UC-79Tr (Structural and Component Materials Development)

☆U.S. GOVERNMENT PRINTING OFFICE: 1982-646-055/199